Earth Science Research; Vol. 5, No. 2; 2016
ISSN 1927-0542 E-ISSN 1927-0550
Published by Canadian Center of Science and Education

Geochemistry of Ultramafic to Mafic Rocks in the Norwegian Lapland: Inferences on Mantle Sources and Implications for Diamond Exploration

Pavel K. Kepezhinskas[1], Glenn M.D. Eriksen[1] & Nikita P. Kepezhinskas[2]

[1] Kimberlitt AS, Tollbugaten 24, Oslo, Norway

[2] Department of Geological Sciences, University of Florida, Gainesville, Florida, USA

Correspondence: Pavel K. Kepezhinskas, Kimberlitt AS, Tollbugaten 24, Oslo, Norway. Tel: 1-813-504-0800. E-mail: pavel_k7@yahoo.com

Received: May 23, 2016 Accepted: July 5, 2016 Online Published: July 28, 2016

doi:10.5539/esr.v5n2p148 URL: http://dx.doi.org/10.5539/esr.v5n2p148

The research is financed by Kimberlitt AS.

Abstract

Geology of the Norwegian Lapland is dominated by diverse Archean crystalline basement complexes superimposed with Proterozoic greenstone belts. Isotopic dating of detrital zircons from basement gneisses in the Kirkenes area establishes presence of Early Archean (3.69 Ga) crustal component as well as three major episodes of crustal growth at 3.2 Ga, 2.7-2.9 Ga and 2.5 Ga. Precambrian terranes are intruded by ultramafic-mafic dikes and sills that range in composition from komatiites and ultramafic-mafic lamprophyres to high-Mg basalts and low-Ti subalkaline basalts. Geochemical characteristics of these rocks fall into three principal groups: 1) enriched compositions with high Nd, Nb, Hf, Zr and Th concentrations and elevated La/Th and Nb/Th coupled with low La/Nb, Ba/Nb and U/Nb ratios; 2) compositions depleted in Th, Hf and Nb together with low LREE/HFSE (such as La/Nb) and LILE/HFSE (such as Ba/Nb and U/Nb) ratios; 3) transitional group clearly identified by marked depletions in Ti, Nb and Ta contents coupled with enrichment in Th and U and other large-ion lithophile elements (LILE). These geochemical characteristics are interpreted within the framework of two principal source models: 1) derivation of parental ultramafic-mafic melts from multiple mantle sources (depleted to enriched) inherited from Archaean lithospheric tectonics and 2) a single primitive mantle source which underwent several depletion and enrichment episodes, at least partially associated with subduction zone processes. Subduction modification of depleted lithospheric mantle was assisted by accretion of subducted sediment to depleted mantle source at Archean, Proterozoic or Early Paleozoic convergent margin. Alkaline ultramafic rocks such as lamprophyres and mica picrites display geochemical characteristics supportive of their origin within stability field of diamond in a deep mantle beneath Norwegian Arctic margin which, together with other lithospheric characteristics, suggests its high potential for hosting economic diamond mineralization.

Keywords: Norwegian craton, komatiites, shoshonitic lamprophyres, subduction, diamonds

1. Introduction

Formation of continental crust and evolution of Archean cratons are among the most important fundamental problems of modern geology. One of the ongoing scientific debates related to this problem focusses on the relative role of plate tectonic processes – such as subduction and production of oceanic crust – on early Earth (Kusky & Polat, 1999; Dhuime et al., 2012; Turner et al., 2014; Kamber, 2015; Nutman et al., 2015). The most controversial issue is whether modern-style subduction operated in Archean (possibly as early as Hadean; Turner et al., 2014), started at the Archean-Proterozoic boundary due to a major planetary reorganization, or was initiated at a certain point in Neoproterozoic (Shirey et al., 2008; Condie & Kroner, 2013). Numerous geologic, petrologic and geochemical studies of the last two decades established existence of fragmented Archean oceanic crust incorporated into cratonic structure (Szilas et al., 2013; Furnes et al., 2015), confirmed presence within Archean terranes of unique rock associations such as boninite-like volcanics (Kerrich et al., 1998; Polat et al., 2002; Smithies et al., 2004; Szilas et al., 2012a), adakites (Polat & Kerrich, 2001; Polat & Kerrich, 2002; Naqvi

et al., 2006; Manikyamba et al., 2008; Manikyamba et al., 2009; Manikyamba et al., 2012), differentiated calc-alkaline series (Polat & Munker, 2004; Wyman, 1999; Smithies et al., 2007; Jenner et al., 2009; Mueller et al., 2010; Szilas et al., 2012b; Kerrich & Manikyamba, 2012) that are believed to be generated within convergent margin settings and led to a discovery of metamorphic rocks indicative of subduction zone thermal regimes (Moyen et al., 2006; Mints et al., 2010; Tappe et al., 2011a; Shchipansky et al., 2012; Sajeev et al., 2013). It has to be acknowledged that certain geochemical discrepancy exists between some of these Archean igneous rock associations and their modern counterparts. For example, although Archean boninite-like (boninitic) rocks do share certain geochemical features (Si enrichment at high Mg# numbers, clear large ion lithophile element enrichments coupled with high field strength element depletions) with modern boninite melts emplaced in frontal arc environments of the Bonin, New Caledonia and Tonga arcs, none of these ancient high-Mg lavas appear to match the extreme depletion manifested in unique chemical compositions of modern boninites. Still, Archean silica-rich, magnesian magmas could be interpreted as have been formed via melting of a fluid-fluxed depleted mantle in a tectonic environment comparable with modern convergent margins (Smithies et al., 2004).

Discovery of Hadean (> 4 Ga) zircons in ancient metasediments from Jack Hills greenstone belt in Australia (Blichert Toft & Albarede, 2008; Harrison, 2009) and of the Eoarchean (4.3 Ga) Nuvvuagittuq greenstone belt in Quebec, Canada (O'Neil et al., 2011; Adam et al., 2013) provided a unique insight into the early (Hadean) processes of crust-mantle differentiation and generation of chemical heterogeneities in the lithospheric mantle (Blichert Toft & Albarede, 1994; Frei et al., 2004; O'Neil et al., 2008; Hoffmann et al., 2010; Polat et al., 2011).

Several recent publications have evaluated rather critically the possible role of plate tectonics in early Earth evolution and introduced several alternative models for Archean tectonics and petrogenesis. Ernst (2009) suggested that "…small, thin lithospheric plates thus were present at the Earth's surface ever since solidification of the magma mush ocean at ~ 4.4 Ga. Only the scales and aspect ratios of the plates, and rates of asthenospheric circulation have changed over geologic time" (Ernst, 2009). In this model, Archean earth was covered by small, hot and, most important, barely subductable platelets which overall structural weakness prevented them from entering a shallow subduction cycle comparable to Phanerozoic arcs and active continental margins. Decompression melting of upwelling mantle plumes generated Archean oceanic crust in a form of thick oceanic plateaus and their melting along the edges of cratonic cores via the shallow return flow created "subduction-like" geochemical signatures in a wide range of Archean magmatic suites such as TTGs, boninites, differentiated calc-alkaline series and low-Ti tholeiites (Ernst, 2009; Bedard et al., 2013). Numerical modelling of formation of basaltic crust on early earth also suggested that gravitation extraction of mafic material in Archean would have led to a protracted depletion of early mantle in incompatible elements. This strong depletion probably resulted in production of thin oceanic crust early on which, even considering high mantle temperatures in the Archean, would substantially increase subductability of Archean oceanic crust and, therefore, overall viability of early plate tectonics (Davies, 2006). Bedard and co-authors developed an original model for early Erath evolution which views behavior of ancient cratonic cores of the continents in a new light (Bedard et al., 2013; Harris & Bedard, 2014a and b). In this set of models, tectonic compression and terrane accretion observed in many areas occupied by Archean crust is created by mobile cratonic nucleii that drift (float) on top of powerful mantle convection currents (plumes) and constantly accrete and subcrete oceanic plateau, portions of other proto-cratons as well as various chemically heterogeneous mantle domains (Bedard et al., 2013; Harris & Bedard, 2014a and b). Subcretion (underthrusting) of thick basaltic oceanic plateaux leads to its partial melting and generation of "subduction-like" geochemical signature which, in this case, has no relationship with subduction process in the *sensu stricto* plate tectonic sense (Bedard et al., 2013). Another process that can account for many geologic and geochemical features observed in Archean terranes includes deformation and magmatism caused by delamination of gravitationally unstable lower crust and lithospheric mantle (Jull & Kelemen, 2001; Zegers & Van Keken, 2001; Foley et al., 2003; Anderson, 2005; Bedard, 2006). Crustal delamination is also an important mechanism of magma production at modern continental margins such as Andes (Kay & Kay, 1993; Tatsumi, 2000).

Extensive diamond research over last 20 years established further links between Archean convergent margin tectonics and diamond formation in major cratons (Shirey et al., 2004; Stachel & Harris, 2008; Shirey & Richardson, 2011). Various diamond suites are carrying geochemical and petrological evidence for subduction and crustal recycling recorded in diamond-hosted mineral inclusions (Ireland et al., 1994; Schulze et al., 2004; Shirey & Richardson, 2011; Logvinova et al., 2015) as well as reflected in their Re-Os (Pearson et al., 1995; Richardson et al., 2001; Westerlund et al., 2006) and C-O-N-S and noble gas isotopic characteristics (Eldridge et al., 1991; Mohapatra & Honda, 2006; Nemchin et al., 2008; Ickert et al., 2013). Current models for diamond formation suggest that diamonds are associated with old (> 2.5 Ga), tectonically stable cratonic cores of the

continents which are characterized by thick lithospheric keel, low heat flow and prolonged periods of tectonic and thermal stability (Shirey at al., 2002; Stachel et al., 2009; Gurney et al., 2010). Diamonds are transported to the surface by kimberlite (Kjarsgaard, 2007) and lamproite (Jaques & Milligan, 2004) magmas (at least in the case of economic diamond deposits) and were also described in a variety of ultramafic-mafic igneous rocks including lamprophyres (Kaminsky, 2007; Smith et al., 2013), arc picrites (Ivanov et al., 2005) and arc-related potassic ultramafic volcanics (Golovko & Kaminsky, 2010). All this suggests that Precambrian convergent margin tectonics along with lower crust delamination (Bedard, 2006) and subcretion of basaltic plateaux (Bedard et al., 2013) not only have played an important role in formation of Archean cratons and early mantle differentiation but was also crucial in creation of unique set of petrologic and geodynamic conditions that generated a wide range of ultramafic-mafic melts in various cratonic settings and, at least in some cases, resulted in a formation of diamond mineralization in continental lithosphere.

The main purpose of this paper is essentially threefold: 1) to present new geochemical data for ultramafic-mafic magmatic rocks from Eastern Finnmark (Arctic Norway); 2) to discuss their possible origins through a multiplicity of their mantle sources with special reference to the role of Archean subduction processes and 3) to briefly evaluate general potential of these mantle-derived ultramafic-mafic magmas to carry an economic diamond mineralization.

2. Geologic Setting

The Norwegian Craton is an Archean cratonic terrane located within the northern part of the Fennoscandian Shield (Fig. 1). It is roughly similar in age, accretionary history and geologic structure to the other cratonic terranes (Kola, Murmansk, Karelian and Norrbotten) of the Nordic Precambrian Province (Gorbatchev & Bogdanova, 1993; Roberts & Nordgulen, 1995). It occupies most of the East Finnmark province in Arctic Norway and is separated from the Kola cratonic terrane in the east (Fig. 1A) by the Paleoproterozoic (2.1-1.7 Ga; Melezhik & Sturt, 1994; Roberts & Nordgulen, 1995) Pasvik-Pechenga Greenstone Belt (PPGB); and from the Karelian craton in the south by the Archean to Paleoproterozoic Belomorian Mobile Belt (3.0-1.8 Ga; Bibikova et al., 2004; Shchipansky et al., 2012) and Lapland Granulite Belt (including Inari Composite Terrane; 3.0-1.9 Ga; Bridgewater et al., 2001; Daly et al., 2001; Korikovsky et al., 2014). Finally, the large-scale frontal thrusts of the Scandinavian Caledonides mark the northern and northwestern boundary of the Norwegian Craton (Fig. 1).

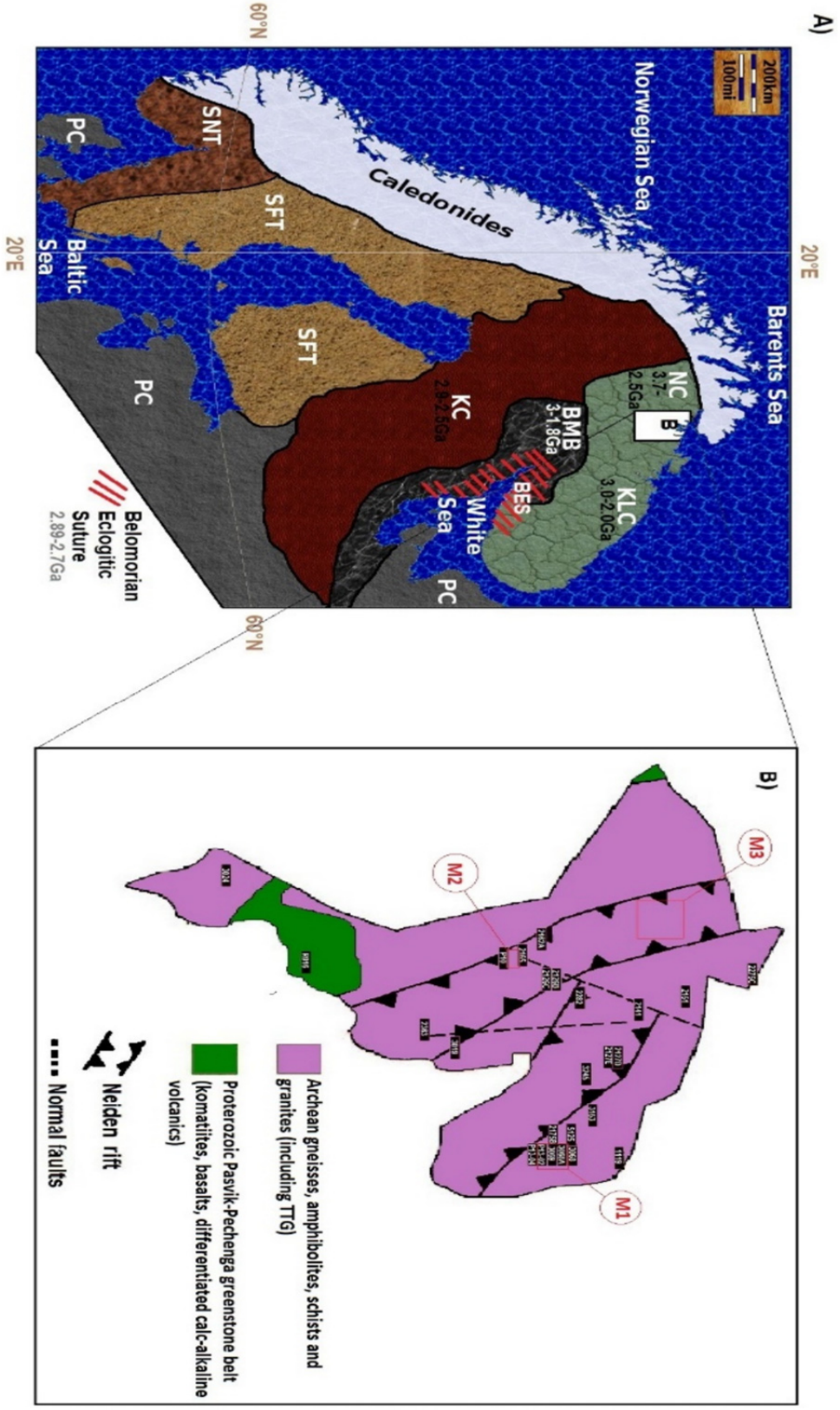

Figure 1. (A) Tectonic setting of the Norwegian craton; (B) Simplified geology of the Sør-Varanger area in eastern Finnmark, Arctic Norway

Note. (A) NC- Norwegian craton, KLC – Kola craton, SKAM – South Kola active margin, BMB – Belomorian mobile belt, KC- Karelian craton. South Kola active margin is marked by 2.89-2.70 Ga-old eclogitic mélange

and associated tonalite-trondhjemite-granite (TTG) rocks (Mints et al., 2010). Ages of individual tectonic units are from: Norwegian craton (Levchenkov et al., 1995; Kepezhinskas, 2011a), Kola craton (Bridgewater et al., 2001; Slabunov et al., 2006), South Kola active margin (Mints et al., 2010), Belomorian mobile belt (Bibikova et al., 2001; Bibikova et al., 2004) and Karelian craton (Bibikova et al., 2001; Nesterova et al., 2011). (B) Main geologic units: KNCT – Kirkenes-Neiden composite terrane (gneisses, amphibolites and garnet amphibolites, mica schists, minor granulites, TTG series, microcline granites and pegmatites), PPGB – Pasvik-Pechenga greenstone belt (pillow-textured komatiites and basalts, ultramafic hyaloclastites, basalt-andesite-dacite-rhyolite metavolcanics). Location of Neiden Rift is shown on the basis of field relationships (distribution of igneous dikes and sills) and regional magnetic and gravimetric data.

The Norwegian Craton is underlain by a thick (45-55 km) continental crust (Azbel et al., 1989; Calcagnile, 1991; Artemieva, 2003; Artemieva, 2007; Artemieva & Tybo, 2008) which is thicker than the average thickness of 42.2 +/- 5.1 km inferred for the East European Craton (Artemieva, 2007). Crustal thickness of the Norwegian Cratonic Terrane (45-55 km) is comparable to the Karelian craton which is characterized by a 47-48 km thick continental crust based on seismic data along the POLAR profile (Gaal et al., 1989). The Norwegian Cratonic Terrane is also characterized by a low thermal gradient of 30-45 mWm^{-2} (Pasquale et al., 2001) typical of other Archean cratons worldwide (Rudnick et al., 1998; Michaut et al., 2009). The crustal roots of the Norwegian Cratonic Terrane, based on the geophysical data and petrological modelling, are considered to be metamorphosed in the high-pressure granulite-facies conditions (Kepezhinskas, 2011a).

Geology of Arctic Norway encompasses a wide variety of tectonic terranes and rock units that mostly consist of Archean supra-crustal complexes and Proterozoic greenstone belts to Neoproterozoic platform sediments of the Norwegian mainland (Roberts & Nordgulen, 1995) but also include fragments of Mesozoic Circum-Arctic large igneous province and Quaternary alkaline basalts of the Svalbard Archipelago as well as an active Beerenberg basaltic volcano on the island of Jan Mayen that last erupted in 1985.

The main geologic units belonging to the Norwegian Craton in the Sør-Varanger area of East Finnmark include the following Archean rocks: 1) an amphibolite-mica schist unit; 2) granite-gneiss unit; 3) granulites and garnet-bearing granites (Fig. 2). Archean rocks are tectonically juxtaposed against Paleoproterozoic greenstone assemblages of the Pasvik-Pechenga belt (Fig. 1B). Archean units contain ultramafic-mafic igneous rocks represented by komatiites, shoshonitic lamprophyres, high- and low-magnesian basalts which form a primary focus of this paper (Fig. 2). Only ultramafic-mafic rocks contained within the Archean geologic units are considered in this study and all of Paleoproterozoic Pasvik greenstones are excluded from the current paper.

Amphibolite-mica schist unit occupies most of the southern part of the Sør-Varanger area (Pasvik River valley) and consists of amphibolites, garnet amphibolites, hornblendites and various amphibole-mica schists present at roughly equal volumes within this unit (Fig. 2). Amphibolites occasionally contain boudines (up to several meters in size) of fine- to coarse-grained gabbro. All rocks of amphibolite-mica schists are impregnated by thin (0.5 to 5 cm) veins of granitic and tonalitic composition.

Granite-gneiss unit occupies the entire northern part of the Sør-Varanger area and encompasses several gneissic units (dubbed Svanvik, Munkelv, Neiden and Jarlsfjord gneisses) which contain abundant tonalite-trondhjemite-granite (TTG) veins, dikes and larger intrusions (Fig. 2). Gneissic complex near Kirkenes includes substantial volumes of banded iron formation rocks (BIF) hosting famous Bjornevatn iron mines which were in intermittent operation since the World War II. Granitic gneisses in Neiden and Bugoyfjord area contain large boudines, blocks and, possibly, dikes of amphibole, amphibole-mica and amphibole-chlorite ultramafic composition. In some areas (near Neiden and along the highway connecting Kirkenes and Tana Bru), these blocks contain variably amphibolized, chloritized and serpentinized ultramafic and mafic rocks.

Granulites and garnet-bearing granites are mostly found to the north and northeast of Kirkenes where they form tectonic blocks and smaller tectonic slivers among felsic gneisses of the granite-gneiss unit (Fig. 2). Granulites are strongly-foliated, commonly two-pyroxene rocks which show no clear evidence for any retrograde metamorphic changes. Granites have intrusive contacts with host granulites and contain abundant garnet porphyrocrysts sometimes accompanied by primary magmatic pyroxene and amphibole.

From the structural viewpoint, Sør-Varanger area is dominated by NW-SE-striking normal and listric faults which are structurally associated with the Neiden paleo-rift (probably formed in late Archean or early Proterozoic time) and associated conjugate shear structures (Fig. 1B). This structural pattern is overprinted with roughly west-east striking normal faults (such as Langfjord fault or Langfjord fracture zone) and related deformations which were most probably generated during the Svecofennian orogeny (1.92-1.77 Ga; Korja et al.,

2006).

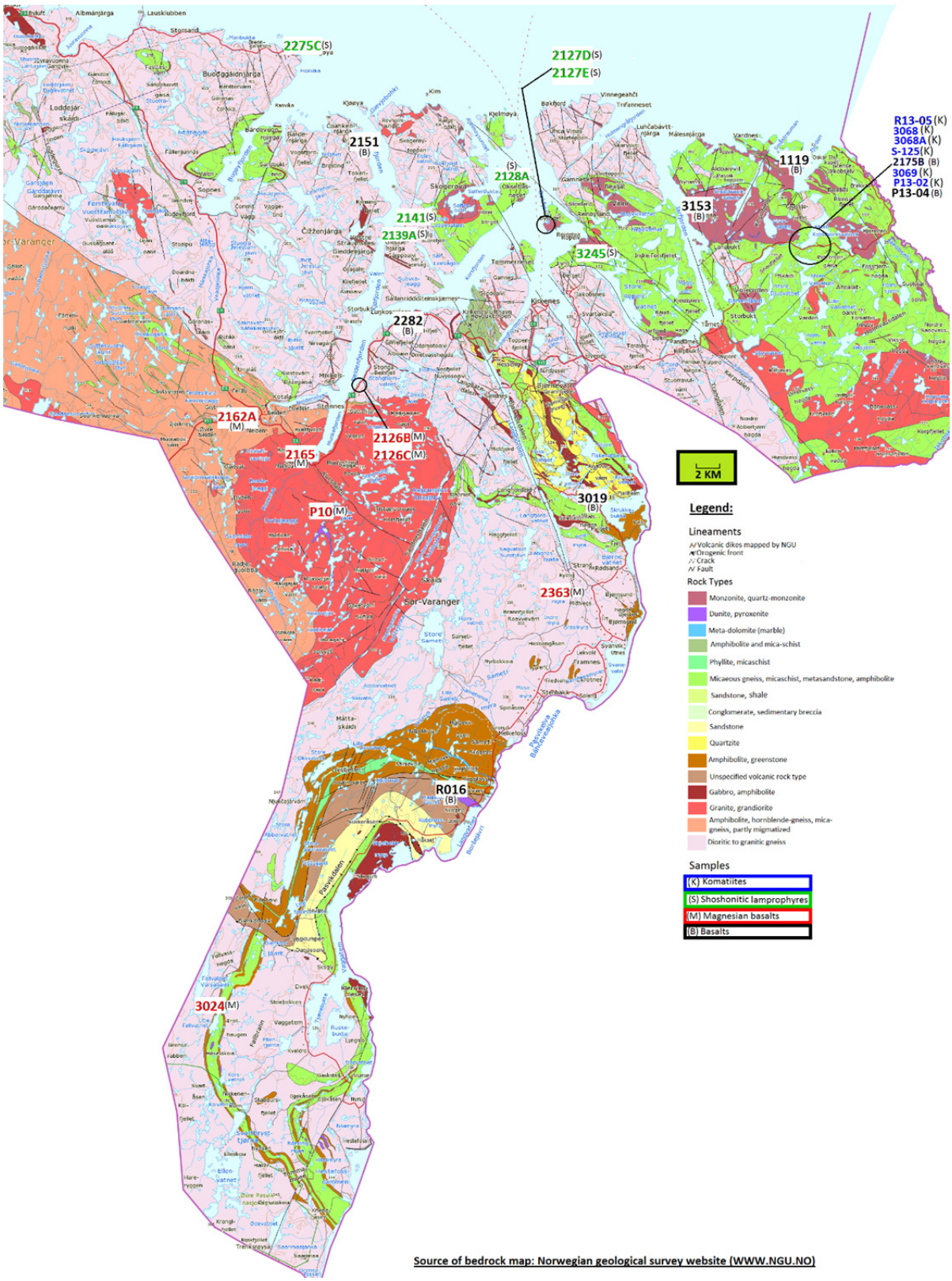

Figure 2. Geological map of the Sør-Varanger area in eastern Finnmark, Arctic Norway (after Roberts & Nordgulen, 1995)

Note. Location of ultramafic-mafic rocks used in this study is indicated using the following color coding scheme: blue – komatiites, green – shoshonitic lamprophyres, red – magnesian basalts, black – basalts.

U-Pb zircon ages for Sør-Varanger terrane gneisses (granite-gneiss unit as described above; Fig. 2) range from 2.95 to 2.7 Ga (Levchenkov et al., 2015). These zircon ages are corroborated by the 2.96-2.78 Ga Sm-Nd model ages for gneisses across the Lapland-Kola terranes which suggested that a major phase of sialic crustal production in the Norwegian craton (as well as within Murmansk and Kola terranes of NW Russia) took place in Late Archean (Timmerman & Daly, 1995). Our U-Pb dating of zircons in felsic gneisses from the Sør-Varanger area revealed a more complex history of their formation and crustal evolution in Eastern Finnmark (Kepezhinskas, 2011a). Some detrital zircons in gneisses from Sør-Varanger yielded ages of 3.69 Ga which probably record one of the oldest crustal events in the Fennoscandian Shield (Kepezhinskas, 2011a). We interpret these ages as reflecting the initial accretion and amalgamation of Eoarchean proto-Fennoscandian cratonic nucleus which was subsequently disintegrated through the processes of Paleoarchean rifting. A substantial population of zircons defines a strong isotopic maximum around 3.2 Ga suggesting that proto-Norwegian craton went through an important crustal accretion episode at the Paleoarchean-Mesoarchean boundary. The majority of our zircon ages from Sør-Varanger gneisses clearly establish a major crustal production stage within the Norwegian Cratonic Terrane between 2.97 and 2.78 Ga which is also consistent with earlier U-Pb and Sm-Nd isotopic studies (Levchenkov et al., 1995; Timmerman & Daly, 1995). Final episode of the Archean crustal accretion and associated deformation is dated at 2.5 Ga (Kepezhinskas, 2011a).

3. Field Relations and Petrography of Ultramafic-Mafic Rocks

Ultramafic-mafic rocks in Eastern Finnmark occur mostly as sills and dikes with minor lava flows (Fig. 3A-D). Dikes show clear cross-cutting relationships with host mafic and felsic gneisses and migmatites (Fig. 3C and D). Komatiites form short and thick (20-30 m) lava flows as well as vein-like injections into the surrounding gneisses (Fig. 3A). Some of the

Figure 3. Field occurrence of ultramafic-mafic dikes and sills in Sør-Varanger area, Eastern Finnmark

Note. A- komatiite lava flow, lower half of outcrop not exposed (sample R13-05). B- blocks of ultramafic rocks in Archean gneisses. C- shoshonitic lamprophyre dike (width-0.7m) in contact with Mesoarchean gneisses and migmatites (sample 2141). D- shoshonitic lamprophyre dike (width-3m) cutting migmatized mafic gneiss (sample 2127D).

thicker komatiitic lava flows are clearly differentiated with well-defined internal cumulate zones and fine-grained flow margins/chilled zones. Dikes also exhibit well-defined chilled margins ranging from 0.5 to 50-60 cm dependent on the overall dike width (Fig. 3C; Fig. 3D). Some thicker (2-50 m) ultramafic and basaltic sills display an internal zoning with coarse- to medium-grained pyroxenitic to gabbroic central parts and medium- to fine-grained basaltic chilled margins. Komatiites occasionally form branching injections into Archean gneisses which typically have thicknesses of 0.5 to 5 cm. From the structural

viewpoint, ultramafic-mafic dikes exhibit predominant NW-SE directions (Fig. 4) which is coincident with the overall orientation of Neiden paleo-rift as illustrated in Figure 1B. Location of Neiden paleo-rift is based on the shape and outline of regional negative gravity anomaly as well as structural peculiarities of underlying Archean basement complexes. The dominant NW-SE orientation of dikes is combined with prominent west-east-striking dike directions (Fig. 4) which is also supported by widespread development of W-E-trending normal faulting in the area. While NW-SE dike orientations may reflect Precambrian or Paleozoic continental break-up and rifting, the W-E-trending dikes are possibly related to a later-stage tectonic processes (Torsvik et al., 1996).

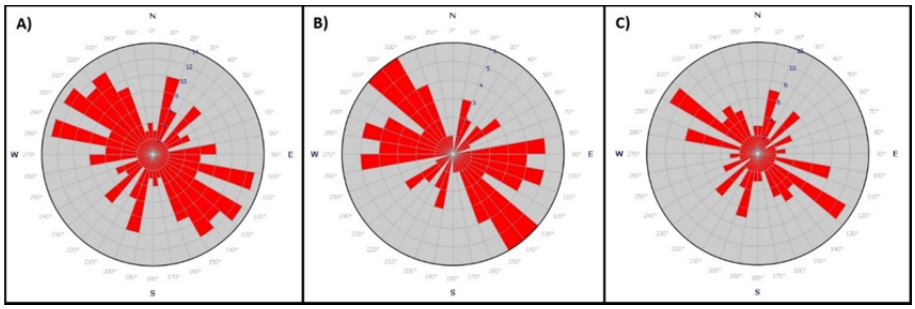

Figure 4. Preferred ultramafic-mafic dike orientations based on field observations and strike measurements

Note. A – the entire dike population for Sør-Varanger area; B – only dikes located west of Kirkenes; C – only dikes located east of Kirkenes.

In this section as well as the geochemical section below we use the following order to describe ultramafic-mafic rocks from the Sør-Varanger area: 1) komatiites, 2) shoshonitic lamprophyres, 3) magnesian basalts and 4) variably fractionated basalts. Although this order of description is somewhat arbitrary, we attempt to generally follow the decreasing MgO content of magmatic rocks in our petrographic and geochemical groupings and classifications.

Komatiites are porphyritic to poikiloblastic rocks (Tab. 1) with subhedral-euhedral phenocrysts of olivine, clinopyroxene and orthopyroxene. Brown mica (phlogopite) is present occasionally (Fig. 5A) along with pargasitic amphibole. Both hydrous mineral phases frequently form small anhedral to euhedral grains which appear to be cementing olivine-pyroxene mineral aggregates (Fig. 5A). Olivine is a dominant mineral phase and occasionally is replaced by patchy

serpentine, saponite, chlorite or iddingsite. Orthopyroxene forms large (5-8 mm) crystals locally showing rimming by or integrowth with zoned prismatic plagioclase. Orthopyroxene poikiloblasts frequently contain olivine and chromite inclusions which texturally appear to represent near-liquidus crystallization phases (Fig. 5A). Clinopyroxene is chrome diopside with high Cr contents (up to. 1.8 wt. % Cr_2O_3) and low Al concentrations (typically < 3 wt. % of Al_2O_3). Plagioclase belongs to calcic bitownite-anorthite series.

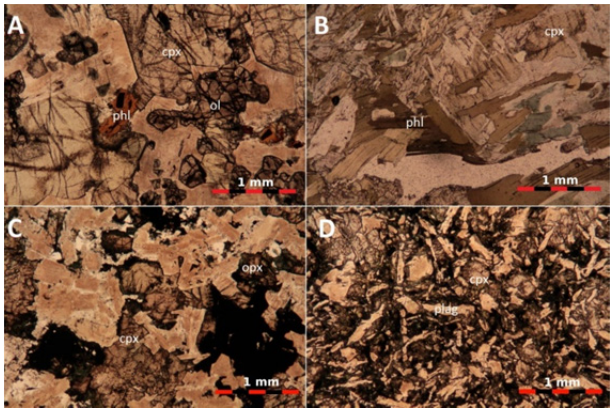

Figure 5. Representative microphotographs of thin sections of the ultramafic-mafic igneous rocks from Sør-Varanger area

Note. A- komatiite lava flow (massive part of a thick lava unit, sample 3069); B- shoshonitic lamprophyre (sample 2128A); C- magnesian basalt (sample 1122A); D- plagioclase-clinopyroxene-phyric basalt (sample r13-12).

Table 1. Petrographic features and phenocryst assemblages in ultramafic-mafic rocks from Sør-Varanger area (Arctic Norway)

Rock types	Primary textures	Phenocryst assemblages	Additional features
Komatiites	Porphyritic, phaneritic (in central parts of thicker lava flows, sills and dikes), aphanitic (within chilled marins of dikes and sills)	Ol-cpx, ol-cpx-opx,ol-opx-cpx-amph, ol-opx-amph, ol-cpx-phl, ol-cpx-opx-phl	Cr-diopside and enstatite megacrysts; sub-liquidus chromite inclusions in olivine and phlogopite; olivine inclusions in orthopyroxene; rare groundmass plagioclase; accessory chromite, Mg-spinel, Ti-magnetite and Ti-Cr-magnetite
Shoshonitic lamprophyres	Porphyritic, poikiloblastic, globular (carb-mt), in rare cases phaneritic (parts of larger shallow intrusions)	Ol-cpx-phl, ol-cpx-amph-phl-plag, ol-opx-cpx-amph, ol-cpx-phl-pl, cpx-opx-amph, cpx-opx-amph-phl,	Primary magmatic calcite; Amphibole, phlogopite and calcic plagioclase megacrysts; plagioclase megacrysts are commonly strongly resorbed; zoned amphibole and phlogopite; Spinel and phlogopite inclusions in amphibole; carbonate-magnetite globular segregations
Magnesian basalts	Porphyritic	Ol-cpx-amph-pl, cpx-amph-phl-pl, cpx-amph	Zoned plagioclase megacrysts; spinel inclusions in plagioclase
Basalts	Porphyritic	Cpx-opx-pl, cpx-pl, ol-cpx-pl	Skeletal plagioclase laths; clinopyroxene inclusions in plagioclase; plagioclase with frequent oscillatory zoning

Note. Mineral abbreviations: ol- olivine, cpx- clinopyroxene, opx- orthopyroxene, pl- plagioclase, amph- amphibole, phl- phlogopite, carb- carbonate, mt- magnetite.

Shoshonitic lamprophyres are typically characterized by porphyritic, poikilitic and phaneritic (in thicker dikes) textures (Tab. 1). Some lamprophyric dikes exhibit ocellar textures which are common for a wide range of lamprophyric rocks with ocelli being replaced by secondary minerals such as albite, calcite and hydromica. Typical phenocrystic assemblages include phlogopite, amphibole, olivine, clinopyroxene, orthopyroxene and plagioclase in various modal proportions (Fig. 5B). Shoshonitic lamprophyres commonly carry large (up to 1 cm)

amphibole and phlogopite megacrysts which occasionally display clear optical zoning. Large (up to 1 cm in length) laths of plagioclase display intense zoning and contain frequent inclusions of euhedral (magmatic?) epidote. Amphiboles commonly contain inclusions of non-deformed euhedral mica and spinel. Some larger mica crystals (sample 2128A, Fig. 5B) exhibit visible kink bending due to plastic deformation during magmatic crystallization and magma transport. Amphibole megacrysts are partially replaced by secondary chlorite and tremolite (Fig. 5B). Both amphiboles (with an exception of secondary tremolite) and phlogopites are interpreted as primary magmatic phases. Olivines are replaced with serpentine-antigorite aggregates, while mica is variably altered into a fine aggregate of hydromica, secondary feldspar and chlorite. Some lamprophyric dikes contain magmatic carbonate which form calcite-magnetite ocelli suggesting that primary shoshonitic lamprophyre magma was probably carbonate-saturated.

Magnesian basalts (picrobasalts) exhibit aphyric and porphyritic textures composed of olivine, clinopyroxene and plagioclase phenocrysts (Tab. 1; Fig. 5C). Some magnesian basaltic dikes carry large (0.5-1.0 cm) amphibole megacrysts that contaim spinel and plagioclase inclusions. Large euhedral plagioclase crystals (megacrysts?) also contain inclusions of opaque spinel (Fig. 5C). Both amphibole and plagioclase grains exhibit optical zoning which is further emphasized by zone distribution of fluid and melt inclusions. Secondary alteration is limited to partial replacement of amphibole with chlorite and tremolite and plagioclase with fine-grained hydromica-albite aggregate.

Basalts form dikes, sills and rare lava flows with distinct columnar jointing. They display both aphyric and porphyritic textures made up mostly with clinopyroxene and plagioclase with minor olivine and/or orthopyroxene (Tab. 1; Fig. 5D). Clinopyroxene forms at least two generations of euhedral to subhedral phenocrysts (with larger – up to 2-3 mm – phenocrysts exhibiting clear optical zoning) and is also found in basaltic groundmass (Fig. 5D). Plagioclase is observed as elongated crystals (Fig. 5D) which in some samples display features of skeletal (dendritic) growth suggesting quick crystallization of basaltic magma upon emplacement in the upper crust. Plagioclase frequently contains inclusions of clinopyroxene and opaque minerals and occasionally displays a well-defined oscillatory zoning.

4. Geochemistry of Ultramafic-Mafic Rocks

Major (wt. %) and trace (ppm) element concentrations in ultramafic-mafic rocks from Sør-Varanger area were determined at the Acme Analytical Laboratories, Vancouver, Canada and are presented in Tables 2 through 5. Details of analytical methods are summarized in Eriksen (2013).

All volcanic rocks in this study display various degrees of secondary alteration (see section on Petrography of Ultramafic-Mafic Rocks). Therefore, it is necessary to briefly evaluate potential effects of secondary processes on trace element geochemistry of ultramafic-mafic rocks from the Sør-Varanger area. Incompatible trace element distributions (for elements which are potentially mobile during secondary alteration processes such as Rb, Cs, Sr, Ba and U) show no correlation with the loss on ignition (LOI) contents in all ultramafic-mafic rocks presented in this paper (Eriksen, 2013). Also, most incompatible elements and their ratios display systematic variations with MgO content of Sør-Varanger rocks which are consistent with primary magmatic processes (for example, crystal fractionation) rather than trace element mobility during hydrothermal alteration.

Komatiites are characterized by high MgO contents (20-30 wt. %; Tab. 2) which are coupled with elevated CaO and Al_2O_3 concentrations. Based on CaO-Al_2O_3-TiO_2 relationships (especially Al_2O_3/TiO_2 ratios of 18.0-21.3; Tab. 2; Fig. 6), komatiites from Sør-Varanger belong to the Al-undepleted sub-type of komatiitic rocks (Nesbitt et al., 1979). Sør-Varanger komatiites display Al_2O_3/TiO_2 ratios close to a value typical of primitive mantle (~22; McDonough & Sun, 1995; Robin Popieul et al., 2012). Al-undepleted komatiites – such as proto-type komatiite lavas from a classical Komati River section of the Barberton greenstone belt – are interpreted as partial melts from a previously depleted, shallow to intermediate mantle source upon exhaustion of garnet in the melting residue (Robin Popieul et al., 2012). Al_2O_3/TiO_2 ratios in Al-depleted komatiites are around 12 and for Al-enriched komatiites - around 30 (Fig. 6) suggesting that both composition of their mantle sources as well as melting conditions

Table 2. Major (wt. %) and trace (ppm) element concentrations in representative komatiites

Sample	P13-02	3069	S-125	3068	3068A	R13-05
SiO_2	42.62	47.32	46.69	42.5	45.3	45.36
TiO_2	0.27	0.41	0.42	0.31	0.42	0.37
Al_2O_3	5.75	8.61	8.29	5.59	7.65	7.57

Cr_2O_3	0.557	0.424	0.451	NA	NA	0.516
Fe_2O_3	11.16	11.55	11.64	11.25	12.33	11.76
MnO	0.16	0.18	0.17	0.14	0.17	0.18
MgO	28.73	21.68	23.49	28.79	23.62	24.14
CaO	4.81	7.06	6.64	4.76	6.25	5.81
Na_2O	0.47	1.11	1.04	0.47	0.88	0.84
K_2O	0.14	0.29	0.20	0.14	0.21	0.20
P_2O_5	0.03	0.04	0.05	0.04	0.05	0.04
LOI	5.73	1.92	2.11	5.7	2.7	3.60
Total	100.44	100.60	101.19	99.74	99.56	100.37
Al_2O_3/TiO_2	21.3	21.0	19.8	18.0	18.2	20.5
Ni	1493.7	790.8	906.0	1336	797.7	934.5
Co	97.1	83.5	82.3	100.6	95.7	87.6
V	118	148	160	121	162	140
Ba	64	98	88	63	94	77
Sr	71.8	104.7	89.2	67.8	88.9	81.2
Rb	4.5	7.1	5.8	3.3	6.5	6.9
Cs	0.1	0.1	0.3	<0.1	0.4	1.0
Zr	23.6	36.4	33.4	24.4	33.2	30.1
Y	5.7	8.5	9.0	6.0	8.7	7.6
Nb	1.4	1.9	1.4	1.1	1.6	1.5
Ta	<0.1	<0.1	<0.1	<0.1	<0.1	<0.1
Hf	0.6	0.9	0.7	0.6	0.8	1.0
Th	0.4	0.7	0.5	0.3	0.8	0.5
U	<0.1	<0.1	<0.1	<0.1	0.1	<0.1
La	3.2	5.0	5.0	2.9	4.7	4.2
Ce	6.5	10.4	9.2	6.9	10.4	8.7
Pr	0.87	1.32	1.20	0.86	1.32	1.11
Nd	3.9	5.9	5.5	3.4	6.1	5.0
Sm	0.91	1.32	1.19	0.82	1.29	1.02
Eu	0.27	0.41	0.38	0.29	0.41	0.36
Gd	0.89	1.43	1.41	1.02	1.36	1.17
Tb	0.16	0.23	0.22	0.17	0.24	0.20
Dy	1.10	1.55	1.39	1.02	1.49	1.24
Ho	0.22	0.32	0.26	0.22	0.31	0.31
Er	0.56	1.02	0.85	0.64	0.96	0.81
Tm	0.09	0.14	0.13	0.10	0.15	0.13
Yb	0.61	0.88	0.79	0.62	0.88	0.93
Lu	0.10	0.14	0.13	0.10	0.14	0.11
Rb/Nb	3.21	3.74	4.14	3.00	4.06	4.60
Rb/Nd	1.15	1.20	1.05	0.97	1.07	1.38
Zr/Nb	16.86	19.16	23.86	22.18	20.75	20.07
Zr/Hf	39.33	40.44	47.71	40.67	41.50	30.10
Nb/Th	3.50	2.71	2.8	3.67	2.00	3.00
Nb/Lu	14.00	13.57	10.77	11.00	11.43	13.64

Note. NA – not analyzed.

contributed heavily to their bulk chemical compositions (Robin Popieul et al., 2012). Ti concentrations in Sør-Varanger komatiites vary within the range of TiO_2 contents typical of komatiitic magmas, unlike clearly elevated Ti concentrations that were earlier reported for komatiite volcanics in the Karasjok greenstone belt of Eastern Finnmark (Barnes & Often, 1990).

Komatiites are characterized by high MgO contents (20-30 wt. %; Tab. 2) which are coupled with elevated CaO and Al_2O_3 concentrations. Based on CaO-Al_2O_3-TiO_2 relationships (especially Al_2O_3/TiO_2 ratios of 18.0-21.3; Tab. 2; Fig. 6), komatiites from Sør-Varanger belong to the Al-undepleted sub-type of komatiitic rocks (Nesbitt et al., 1979). Sør-Varanger komatiites display Al_2O_3/TiO_2 ratios close to a value typical of primitive mantle (~22;

McDonough & Sun, 1995; Robin Popieul et al., 2012). Al-undepleted komatiites – such as proto-type komatiite lavas from a classical Komati River section of the Barberton greenstone belt – are interpreted as partial melts from a previously depleted, shallow to intermediate mantle source upon exhaustion of garnet in the melting residue (Robin Popieul et al., 2012). Al_2O_3/TiO_2 ratios in Al-depleted komatiites are around 12 and for Al-enriched komatiites - around 30 (Fig. 6) suggesting that both composition of their mantle sources as well as melting conditions contributed heavily to their bulk chemical compositions (Robin Popieul et al., 2012). Ti concentrations in Sør-Varanger komatiites vary within the range of TiO_2 contents typical of komatiitic magmas, unlike clearly elevated Ti concentrations that were earlier reported for komatiite volcanics in the Karasjok greenstone belt of Eastern Finnmark (Barnes & Often, 1990).

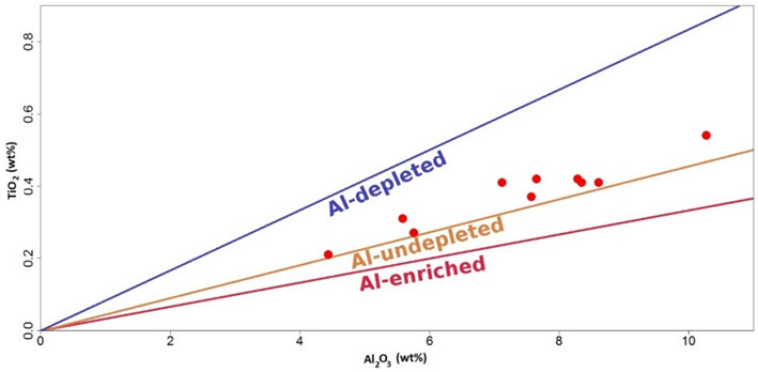

Figure 6. Variations of Al_2O_3 (wt. %) versus TiO_2 (wt. %) in komatiites from the Sør-Varanger area (Arctic Norway)

Note. Al_2O_3/TiO_2 ratios for Al-depleted (Al_2O_3/TiO_2 = 10), Al-undepleted (Al_2O_3/TiO_2 = 22) and Al-enriched (Al_2O_3/TiO_2 = 30) ratios for komatiitic magmas are from Robin Popieul et al. (2012).

Komatiites, magnesian basalts and various differentiated (medium- to low-MgO contents; Tab. 2, 4 and 5) basaltic rocks display moderate increase in Ti, K, Rb, Sr and Th concentrations along with Ti/Zr, Ba/Zr and Nb/Hf ratios with declining MgO which is consistent with widespread fractional crystallization of their parental melts (medium-MgO komatiites?). MgO-trace element covariations suggest that in general komatiites, magnesian basalts and low-Mg basaltic rocks form three separate compositional groups although some magnesian basalts might be related to komatiites through crystal fractionation (Fig. 7).

Trace element compositions of komatiites normalized to primitive mantle (Sun & McDonough, 1995) are shown in Figure 8A. Komatiites form a coherent compositional array characterized by well-pronounced enrichments in large-ion lithophile elements (LILE - Ba and Th) and marked depletions in high-field strength elements (HFSE) such as Ta and Nb (Fig. 8A).

High LILE/HFSE ratios and especially clear depletions of HFSE in respect to LILE and light rare earth elements (negative Ta, Nb, Ti, Zr anomalies in chondrite-normalized patterns) are commonly viewed as geochemical fingerprints of subduction-related magmas (Perfit et al., 1980; Hawkesworth et al., 1994; Thirlwall et al., 1994; Pearce, 2008). This is also consistent with slightly LREE-enriched primitive mantle-normalized rare earth patterns (Fig. 8A) which are typical of mafic and ultramafic melts generated within subduction-zone environments (McCulloch & Gamble, 1991). Subduction origin for komatiites was proposed originally by Allegre (1982) and later supported by additional petrological (Parman et al., 2001) and geochemical (Gurenko & Kamenetsky, 2011) evidence. Although, currently a purely subduction zone origin is not considered to be a dominant model for komatiite petrogenesis (Nesbitt et al., 1979; Barnes & Often, 1990; Puchtel et al., 1999; Robin Popieul et al., 2012), involvement of some subduction-modified mantle sources in formation of Sør-Varanger komatiites cannot be completely ruled out on the basis of geochemical data presented above.

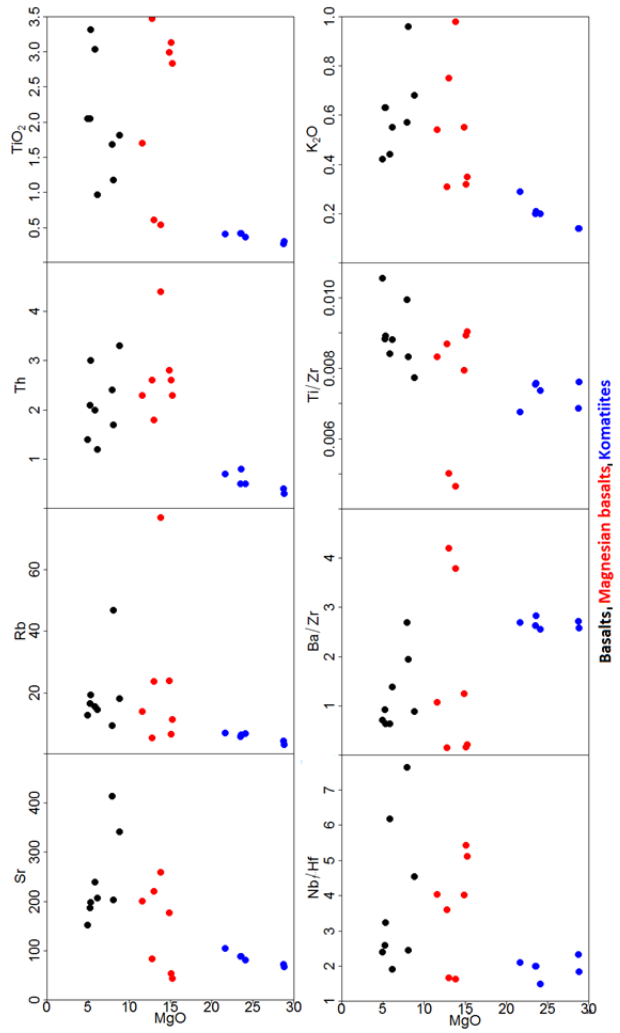

Figure 7. Variations of MgO (wt. %) with TiO_2 (wt. %), K_2O (wt. %), Th (ppm), Rb (ppm), Sr (ppm), Ti/Zr, Ba/Zr and Nb/Hf in komatiites (blue), magnesian basalts (red) and basalts (black) from the Sør-Varanger area

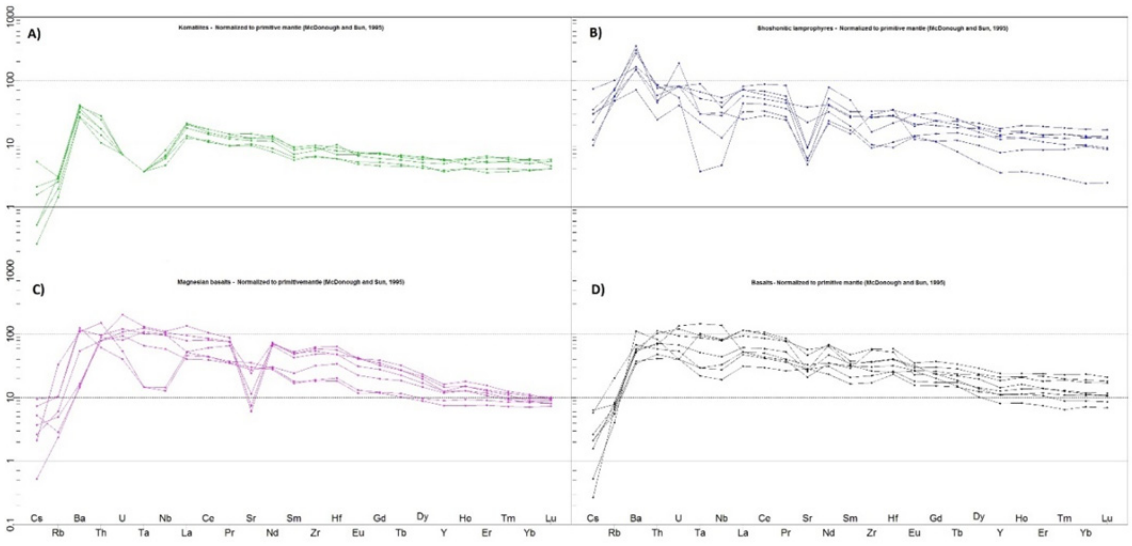

Figure 8. Primitive mantle –normalized trace element compositions of ultramafic-mafic rocks from Sør-Varanger area

Note. A- komatiites; B- shoshonitic lamprophyres; C- magnesian basalts and D- basalts. Normalizing values are from McDonough & Sun (1995).

Shoshonitic lamprophyres are low- to medium-Ti rocks which display a wide range of MgO contents (19-6 wt. %; Tab. 3). They display low N_2O (0.26-1.23 wt. %) and high K_2O (1.69-4.79 wt. %) concentrations coupled with high K_2O/Na_2O ratios (1.4-18.4; Tab. 3) typical of subduction-related (orogenic) shoshonitic magma series (Thompson & Fowler, 1986; Kepezhinskas, 1994; Avanzinelli et al., 2009). Concentrations of K, Ti, Zr, Y and, to a certain extent, Th appear to be generally increasing with decreasing MgO content (Tab. 3) reflecting crystal fractionation of primary shoshonitic magmas. Crystal fractionation is an important petrogenetic process which governs both mantle and crustal evolution of shoshonite rock series which commonly results in a formation of nearly continuous range of K-enriched rock compositions from mafic absarokite through intermediate shoshonite (K-enriched basaltic andesite) and banakite (K-enriched andesite) to most evolved (essentially, dacitic in composition) latite (Meen, 1989). On the shoshonite discrimination diagrams of Kepezhinskas (1994), Sør-Varanger lamprophyres plot both into the fields of low-Ti and high-Ti shoshonites (Fig. 9A and B).

Low-Ti shoshonites are produced largely within subduction zone environments such as volcanic arcs (Marianas, Greece, Aeolian Islands, Fiji) and active continental margins (Andes and Kamchatka). High-Ti shoshonitic magma series are associated with extension (rifiting) of syn-collisional and post-collisional orogens and were probably derived from subduction-modified mantle sources left behind after termination or lateral migration (slab rollback) of an active subduction zone (Alboran rift and Morrocan margin, Central Italy, Corsica, West Alps, Central Asian and Chinese orogenic belts; Kepezhinskas, 1994; Gill et al., 2004; Conticelli et al., 2009).

Primitive mantle-normalized trace element characteristics of shoshonitic lamprophyres in the Sør-Varanger area also support their dual origin and existence of two geochemical types of shoshonites in Eastern Finnmark (Fig. 8B). All Sør-Varanger shoshonites exhibit clear enrichment in Ba and U which is a typical signature of subduction-modified mantle source (Kay, 1980; McCulloch & Gamble, 1991; Hawkesworth et al., 1994; Pearce, 2008). They also display variable depletion in HFS elements (Nb and Ta; Fig. 8B). Trace element data as well as major element compositions of shoshonitic lamprophyres suggest spatial co-existence of two types – high-Ti and low-Ti - of shoshonitic magma although their isotopic ages are currently unknown and field temporal relationships are enigmatic. We will attempt to shed some light on possible petrogenetic and tectonics significance of shoshonitic lamprohyres in Sør-Varanger province in the Discussion section below.

Table 3. Major (wt. %) and trace (ppm) element concentrations in representative shoshonitic lamprophyres

Sample	2139A	2128A	2127D	2275C	3245	2127E	2141
SiO_2	50.4	47.1	49.7	48.5	50.8	51.32	47.1
TiO_2	0.38	0.72	1.69	0.58	1.72	1.47	1.48
Al_2O_3	6.75	7.79	8.61	8.58	14.33	14.43	14.93
Cr_2O_3	NA	NA	NA	NA	NA	0.007	NA
Fe_2O_3	8.07	10.55	13.59	12.57	14.09	16.08	16.85
MnO	0.12	0.17	0.18	0.20	0.12	0.18	0.20
MgO	19.19	19.23	13.19	14.29	7.16	6.38	7.30
CaO	9.15	7.82	7.87	10.86	1.28	3.24	4.28
Na_2O	0.49	0.37	0.57	1.23	0.99	0.59	0.26
K_2O	2.79	3.25	2.86	1.69	3.38	4.53	4.79
P_2O_5	0.20	0.30	0.14	0.05	0.13	0.13	0.15
LOI	2.0	2.3	1.4	1.2	5.3	1.49	2.5
Total	99.56	99.58	99.80	99.83	99.34	99.91	99.88
K_2O/Na_2O	5.7	8.8	5.0	1.4	3.4	7.7	18.4
Ni	156.5	406.4	261.2	217.0	91.7	50.0	83.4
Co	58.1	65.1	75.6	68.4	61.6	47.3	44.6
V	112	195	273	236	412	346	343
Ba	640	852	363	171	355	395	730
Sr	157.6	63.8	61.9	34.0	43.1	39.3	272.5
Rb	126.7	160.5	111.0	108.8	131.3	230.0	170.7
Cs	5.6	6.6	5.7	2.2	1.8	14.1	4.2
Zr	36.9	59.0	125.0	32.8	109.4	100.0	101.2

Y	5.5	24.9	18.5	20.6	11.4	21.8	27.3
Nb	1.1	9.1	10.8	3.0	7.5	12.9	6.7
Ta	<0.1	1.2	0.7	0.3	0.4	0.9	0.4
Hf	0.9	2.2	3.5	1.1	3.6	2.8	2.9
Th	2.4	1.4	1.7	0.7	1.3	2.5	2.2
U	0.4	0.6	0.6	0.3	1.4	0.6	0.6
La	10.4	19.3	17.1	7.6	5.8	16.9	13.5
Ce	25.8	53.8	41.5	20.2	17.2	36.2	31.4
Pr	3.36	7.81	5.27	2.48	2.21	4.57	4.10
Nd	14.6	35.7	23.6	10.5	9.5	18.5	19.1
Sm	2.83	7.29	4.77	2.44	2.12	3.88	4.07
Eu	0.73	1.63	1.57	0.76	0.66	1.16	1.07
Gd	2.13	6.08	4.61	2.85	2.18	3.87	4.64
Tb	0.27	0.89	0.72	0.54	0.41	0.65	0.82
Dy	1.22	4.46	3.74	3.17	2.32	4.26	5.16
Ho	0.20	0.86	0.68	0.68	0.44	0.81	1.06
Er	0.53	2.21	1.72	2.05	1.29	2.23	3.02
Tm	0.07	0.35	0.24	0.30	0.20	0.35	0.44
Yb	0.38	2.15	1.54	2.01	1.48	2.07	2.73
Lu	0.06	0.32	0.21	0.30	0.20	0.30	0.41
Rb/Nb	115.18	17.64	10.28	36.27	17.51	17.83	6.25
Rb/Nd	8.68	4.50	4.70	10.36	13.82	12.43	41.63
Zr/Nb	33.55	6.45	11.57	10.93	14.59	7.75	15.10
Zr/Hf	41.00	26.8	35.70	29.82	30.39	35.71	34.90
Nb/Ta		7.58	15.43	10.00	18.75	14.33	16.75
Nb/Th	0.46	6.5	6.35	4.29	5.77	4.61	3.05
Nb/U	2.75	15.16	18.00	10.00	5.36	21.50	11.17
Nb/La	0.11	0.47	0.63	0.39	1.29	0.76	0.50
Nb/Lu	18.33	28.44	51.43	10.00	37.5	43.00	16.34
Th/U	6.00	2.33	2.83	2.33	0.93	4.17	3.67

Note. NA – not analyzed.

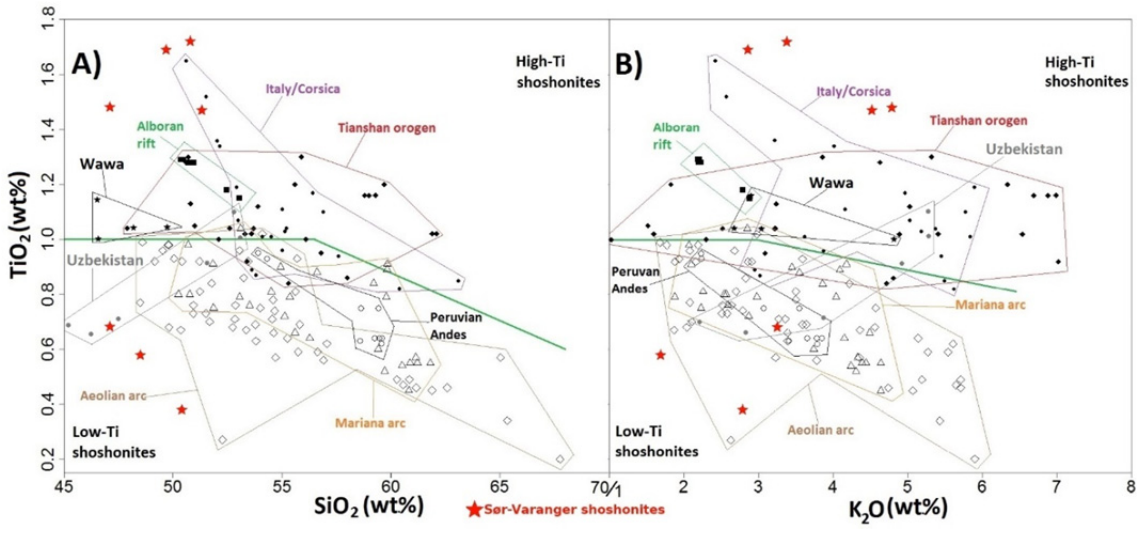

Figure 9. Geochemical diagrams for the tectonic interpretation of shoshonite magma series (Kepezhinskas, 1994)

Note. A- TiO2 (wt. %) vs. SiO2 (wt. %); B- TiO2 (wt. %) vs. K2O (wt. %). Fields for low-Ti (subduction-related arcs) and high-Ti (syn- and post-collisional extensional settings) shoshonites are from Kepezhinskas (1994). Fields for representative low-Ti shoshonites: Peruvian Andes (Kontak et al., 1986), Mariana arc (Bloomer et al., 1989; Sun et al., 1998; Sun & Stern, 2001) and Aeolian arc (Vulzini and Stromboli; De Astis et al., 2013; Francalani et al., 2013). Fields for representative high-Ti shoshonites: rifted Alboran margin of Morocco (Gill et

al., 2004), syn-collisional West Tianshan orogen, China (Yang et al., 2012), post-collisional magmatic associations of Tuscany and Campania, Italy and Corsica, France (Conticelli et al., 2009; Melluso et al., 2014).

Magnesian basalts from Sør-Varanger area are characterized by high TiO_2 of 1.70 to 3.47 wt.% coupled with uniformly low Al_2O_3 content of 6.64 to 7.89 wt.% (Tab. 4) with an exception of two compositions – samples 2162A and 2165 – which display low TiO_2 and high Al_2O_3 concentrations (0.61 and 0.54 wt.% and 12.33 and 11.72 wt.% respectively; Tab. 4). All magnesian basalts exhibit low K_2O contents (< 1 wt. %; Tab. 4) and generally low alkali (K+Na) concentrations. MgO contents vary from approximately 10 to 16 wt.% (Tab. 4) and are reasonably well correlated with variations in Ni, Cr and Co. Magnesian basalts from Sør-Varanger area display clear enrichment in Ba, Sr and Rb coupled with depletion in Zr,Y, Nb and Ta from high-Ti to low-Ti compositional varieties (Tab. 4). These geochemical distinctions clearly establish existence of two types of primitive basalts in the Norwegian Lapland: 1) low-Al, HFSE-enriched and LILE-depleted and 2) high-Al, HFSE-depleted and LILE-enriched.

Primitive mantle-normalized magnesian basalt compositions from Sør-Varanger area exhibit a compositional range from HFSE (Nb and Ta) depleted to undepleted patterns and slightly enriched patterns accompanied by variable beahviour of lithophile elements as Ba, U and Sr (Fig. 8C). HFSE variations cover a range of under 20 x primitive mantle to over 100 x primitive mantle values (Fig. 8C) suggesting major chemical heterogeneity of the respective mantle sources. This is further supported by variable (sometimes substantial) variations in primitive mantle-normalized Ba, Th, U and La values (Fig. 8C) which is also consistent with existence of diverse lithospheric mantle sources.

Table 4. Major (wt. %) and trace (ppm) element concentrations in representative magnesian basalts

Sample	2126B	2126C	P10	3024	2363	2162A	2165
SiO_2	43.80	42.46	44.25	45.3	49.3	50.8	50.3
TiO_2	2.83	3.13	2.99	3.47	1.70	0.61	0.54
Al_2O_3	7.17	7.89	6.64	7.89	9.29	12.33	11.72
Cr_2O_3	0.144	0.159	0.161	NA	NA	NA	NA
Fe_2O_3	16.36	17.53	17.73	18.42	14.14	10.49	10.18
MnO	0.37	0.34	0.21	0.19	0.19	0.16	0.16
MgO	15.20	15.11	14.84	12.74	11.58	12.98	13.81
CaO	9.47	9.40	9.29	9.45	8.99	8.59	7.87
Na_2O	0.26	0.53	1.08	1.09	2.32	1.90	1.92
K_2O	0.35	0.32	0.55	0.31	0.54	0.75	0.98
P_2O_5	0.25	0.27	0.28	0.09	0.16	0.11	0.10
LOI	3.46	3.13	1.21	0.7	1.3	1.2	1.9
Total	99.68	100.28	99.28	99.64	99.46	99.90	99.44
Ni	524.3	477.8	171.6	63.6	141.7	176.3	101.8
Co	82.7	92.2	79.2	79.9	63.1	64.2	61.8
V	275	340	335	376	280	189	193
Ba	40	35	281	37	132	306	264
Sr	44.1	53.8	177.1	83.0	200.4	220.0	258.7
Rb	11.4	6.6	23.9	5.4	13.9	23.8	76.9
Cs	0.7	1.0	1.4	0.1	0.5	1.8	0.4
Zr	187.6	209.8	225.4	239.2	122.4	72.8	69.6
Y	19.8	23.0	19.8	25.6	18.7	14.1	11.8
Nb	25.6	26.6	23.3	23.8	14.1	3.5	3.1
Ta	1.7	1.8	1.4	1.5	0.9	0.2	0.2
Hf	5.0	4.9	5.8	6.6	3.5	2.1	1.9
Th	2.3	2.6	2.8	2.6	2.3	1.8	4.4
U	0.8	1.5	0.9	0.6	0.7	0.3	0.4
La	22.8	32.3	18.8	12.5	9.6	12.3	10.9
Ce	53.3	65.0	49.6	37.4	24.1	27.5	27.2
Pr	7.09	8.26	7.06	6.12	3.24	3.28	3.47
Nd	30.3	33.8	33.1	31.9	14.0	12.7	13.3

Sm	6.34	7.39	7.25	7.80	3.62	2.50	2.67
Eu	1.75	2.42	2.29	2.33	1.27	0.74	0.66
Gd	5.58	6.44	6.99	7.74	3.97	2.42	2.36
Tb	0.81	0.97	0.99	1.16	0.67	0.42	0.37
Dy	4.2	5.28	4.82	5.71	3.60	2.39	2.19
Ho	0.70	0.82	0.83	0.98	0.70	0.51	0.41
Er	1.71	2.12	2.04	2.48	1.88	1.45	1.22
Tm	0.23	0.29	0.27	0.31	0.24	0.21	0.18
Yb	1.35	1.72	1.42	1.80	1.56	1.43	1.14
Lu	0.20	0.25	0.20	0.23	0.24	0.22	0.18
Rb/Nb	0.45	0.43	1.03	0.23	0.99	6.80	24.81
Rb/Nd	.38	0.20	0.72	0.17	0.99	1.87	5.78
Zr/Nb	7.33	7.89	9.67	10.05	8.68	20.8	22.45
Zr/Hf	37.52	42.82	38.86	36.24	34.97	34.67	36.63
Nb/Ta	15.06	14.78	16.64	15.87	15.67	17.50	15.50
Nb/Th	11.13	10.23	8.32	9.15	6.13	1.94	0.70
Nb/Lu	128	106.4	116.5	103.48	58.33	15.90	17.22
Th/U	2.88	1.73	3.11	4.33	3.29	6.00	11

Note. NA – not analysed.

Basaltic rocks from the Sør-Varanger area display substantial chemical variations best exemplified by co-existence of high-Ti (TiO_2>2 wt.%) and low-Ti (TiO_2<1.wt.%) compositions with practically continuous range of Ti concentrations mimicked, at least to a certain extent, by Al contents (Tab. 5). All basaltic dikes and sills in Sør-Varanger area have low potassium contents (<1 wt. K_2O; Tab. 5) and high Na/K ratios defining them from bulk compositional viewpoint as tholeiitic basalts (perhaps with an exception of rare Al-enriched and Ti-depleted compositions such as samples 3153 and 3019 in Table 5). Sør-Varanger basalts exhibit substantial variations in Rb, Sr, Zr, Y and especially Nb and Ta variations (Tab. 5) suggesting their derivation from multiple lithospheric mantle sources (somewhat similar to the compositional variations in magnesian basaltic suite – see Tables 4 and 5 for comparison).

Table 5. Major (wt. %) and trace (ppm) element concentrations in representative basalts

Sample	R016	P13-04	1119	2175B	2151	2282	3153	3019
SiO_2	47.14	49.12	47.43	48.84	48.9	49.4	50.1	51.3
TiO_2	3.03	3.31	1.68	2.05	1.81	2.05	1.18	0.97
Al_2O_3	12.06	12.21	12.70	13.21	12.05	12.65	13.95	14.01
Cr_2O_3	0.003	0.017	0.056	0.013	NA	NA	NA	NA
Fe_2O_3	16.59	17.81	16.38	16.66	13.97	17.19	13.39	13.05
MnO	0.20	0.25	0.26	0.20	0.18	0.23	0.14	0.20
MgO	5.80	5.30	7.89	4.90	8.79	5.22	8.07	6.13
CaO	9.10	8.46	7.00	8.72	7.86	9.03	6.97	9.98
Na_2O	3.53	2.50	4.06	2.02	2.57	2.27	2.08	2.56
K_2O	0.44	0.63	0.57	0.42	0.68	0.63	0.96	0.55
P_2O_5	0.28	0.29	0.20	0.16	0.23	0.18	0.10	0.07
LOI	1.43	0.31	1.88	2.76	2.3	0.8	2.7	1.0
Total	99.61	100.25	100.14	99.97	99.33	99.61	99.63	99.81
Ni	36.1	36.4	112.7	40.7	147.2	35.0	32.3	13.1
Co	57.4	44.1	63.6	48.3	60.0	51.6	48.8	46.7
V	339	427	276	406	237	423	320	291
Ba	138	141	272	83	124	129	165	91
Sr	239.6	198.7	413.7	152.1	340.8	187.0	202.8	207.1
Rb	15.5	19.4	9.3	12.8	18.1	16.5	46.9	14.5
Cs	<0.1	0.3	0.1	0.4	1.2	0.5	1.1	0.4
Zr	215.7	222.4	101.2	116.4	140.4	139.1	85.0	65.9
Y	22.5	37.8	12.7	29.3	17.2	33.1	19.9	17.7

Nb	33.4	19.7	19.9	7.9	19.1	10.6	6.6	4.6
Ta	2.0	1.3	1.4	0.4	1.2	0.7	0.4	0.3
Hf	5.4	6.1	2.6	3.3	4.2	4.1	2.7	2.4
Th	2.0	3.0	2.4	1.4	3.3	2.1	1.7	1.2
U	1.0	0.9	0.3	0.3	0.7	0.5	0.4	0.3
La	12.6	22.6	27.6	12.5	27.6	14.7	11.3	7.4
Ce	31.0	53.1	61.5	26.8	65.7	36.4	25.5	18.3
Pr	3.77	7.20	7.37	3.64	8.03	4.91	3.38	2.47
Nd	16.1	30.9	29.2	16.0	31.7	21.6	14.2	10.7
Sm	4.34	7.10	4.79	4.65	5.61	5.11	3.08	2.45
Eu	1.30	1.99	1.49	1.52	1.80	1.68	1.03	0.89
Gd	4.76	7.44	3.99	5.22	4.69	5.98	3.48	3.06
Tb	0.80	1.22	0.55	0.85	0.68	1.03	0.63	0.53
Dy	4.84	7.17	2.53	5.56	3.37	5.79	3.55	3.07
Ho	0.89	1.32	0.45	1.14	0.62	1.16	0.75	0.62
Er	2.24	3.83	1.20	2.90	1.72	3.47	2.22	1.91
Tm	0.31	0.57	0.16	0.47	0.22	0.49	0.32	0.27
Yb	1.83	3.78	1.16	2.81	1.43	3.08	1.92	1.75
Lu	0.26	0.52	0.17	0.42	0.21	0.45	0.29	0.27
Rb/Nb	0.46	0.98	0.47	1.62	0.95	1.56	7.11	3.15
Rb/Nd	0.96	0.63	0.32	0.80	0.57	0.76	3.30	1.36
Zr/Nb	6.46	11.29	5.09	14.73	7.35	13.12	12.88	14.33
Zr/Hf	39.94	36.46	38.92	35.27	33.43	33.93	31.48	27.46
Nb/Ta	16.70	15.15	14.21	19.75	15.92	15.14	16.50	15.33
Nb/Th	16.70	6.57	8.29	5.64	5.79	5.05	3.88	3.83
Nb/Lu	128.46	37.88	117.06	18.81	90.95	23.56	5.12	17.04
Th/U	2.00	3.33	8.00	4.67	4.71	4.20	4.25	4.00

Note. NA – not analyzed.

Primitive mantle-normalized trace element compositions of basaltic rocks in Sør-Varanger area are listed in Figure 8D. They probably reveal the largest compositional diversity among the ultramafic-mafic rocks from Eastern Finnmark indicated by co-variations of normalized LIL and HFS elements (Fig. 8D). The main difference between various geochemical sub-types of basaltic dikes in Sør-Varanger are LILE (such as Ba, Th and U), HFSE (Nb and Ta) and LREE (La and Ce) elemental ratios. Basaltic compositions appear to form nearly continuous compositional array from Ta-Nb-depleted (relative to primitive mantle) basalts through undepleted to HFSE-enriched varieties (Fig. 8D). Most basalts also display slight, but detectable positive Hf anomaly (sub-chondritic Zr/Hf ratios; Tab. 5) and negative Sr anomaly (plagioclase and possibly amphibole fractionation). Primitive mantle-normalized REE patterns show uniform moderate enrichment of LREE over MREE and HREE (Fig. 8D).

5. Discussion

Variable major and trace element characteristics of ultramafic-mafic rocks from East Finnmark (Arctic Norway) suggest presence of multiple lithospheric sources beneath the Norwegian craton. These mantle heterogeneities may possibly reflect complex patterns involved in accretion of major cratons and involve a number of geodynamic and petrologic processes such as extensive mantle differentiation and mantle-crust interactions, plume-continent interactions, oceanic plateau-arc collisions, oceanic plateau differentiations as well as various subduction processes although the role of subduction in early Earth differentiation is still a subject to vigorous debate (Blichert Toft & Abarede, 1994; Kusky & Polat, 1999; Shirey et al., 2008; Mueller et al., 2010; Kusky et al., 2013; Kamber, 2015). In this paper we attempt to address questions of lithospheric mantle heterogeneity and multiple sources of ultramafic-mafic melts beneath the Norwegian craton as well as possible geodynamic processes that contributed to their formation in the discussion sections below.

5.1 Inferences on Possible Mantle Sources

Major and trace element characteristics of the ultramafic-mafic rocks from Sør-Varanger area can be used to reconstruct chemical composition of their mantle sources. Our preliminary review of their geochemical characteristics presented above suggests that multiple lithospheric mantle sources contributed to the formation of

ultramafic-mafic magmas in Arctic Norway.

A Nd versus Nb graph shows a wide variation in Nd/Nb ratios in ultramafic-mafic igneous rocks in Sør-Varanger (Fig. 10). Most of Sør-Varanger data points are grouped between Nd/Nb ratios of 1 to 4 which characterize the range of depleted (Nd/Nb=4) to enriched (Nd/Nb=1) lithospheric mantle sources (Workman & Hart, 2005; Carlson & Boyet, 2008). Some Sør-Varanger dikes display high Nd/Nb ratios of 15-22 which are similar to LREE/HFSE ratios in the subduction pelagic sediment (represented by clay sediment from the Tonga trench; Nd/Nb=20; Plank & Langmuir, 1998). Sør-Varanger ultramafic-mafic rocks form a nearly continuous compositional array that extends over most of mantle-derived primary magmas from low-Nb/moderate-Nd island arc basalts through less Nb-depleted N-MORBs to enriched MORB varieties and oceanic island basalts (Fig. 10). These chemical variations are consistent with derivation of Sør-Varanger ultramafic-mafic magmas from multiple lithospheric mantle sources ranging from depleted (N-MORB-like) to enriched (OIB-like) mantle which are comparable, at least to a certain extent, to heterogeneous mantle domains recognized under modern mid-oceanic ridges, oceanic plateaus and hot spots as well as subduction-related volcanic arcs.

Ultramafic-mafic rocks from the Sør-Varanger area form a nearly continuous compositional array ranging from rocks with relative low La/Nb (< 2) and U/Nb (< 0.10) to compositions that exhibit high La/Nb (up to 30) and U/Nb (up to 0.60) ratios (Fig. 11) suggesting possible addition of a LILE- and LREE-rich component to their mantle source. This can be either a hydrous fluid (McCulloch & Gamble, 1991; Hawkesworth et al., 1994) or a small-fraction

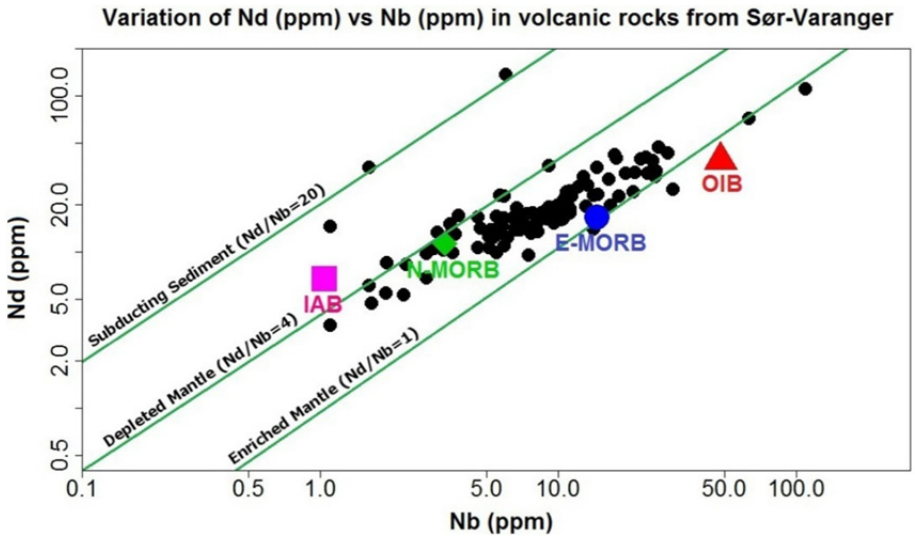

Figure 10. Nd (ppm) versus Nb (ppm) graph for ultramafic-mafic rocks from the Sør-Varanger area

Average Nd and Nb values for island arc basalts (IAB), normal (depleted) mid-ocean ridge basalts (N-MORB), enriched mid-ocean ridge basalts (E-MORB) and ocean island basalts (OIB) are from Niu & O'Hara (2003). Nd and Nb values for depleted mantle are from Workman & Hart (2003) and for enriched mantle – from Carlson & Boyet (2008). Nd/Nb ratio in subducting pelagic sediment is from Plank & Langmuir (1998).

sediment melt (Plank & Langmuir, 1998) both of which are capable of introducing high LILE/HFSE and LREE/HFSE ratios into the lithospheric mantle. Sør-Varanger ultramafic-mafic rocks with relatively low La/Nb and U/Nb ratios appear to be similar to magmas derived from OIB and N-MORB sources (Fig. 11). In fact, nearly a third of Sør-Varanger dikes, sills and lava flows plot into a combined field of oceanic basalts (including both oceanic island and mid-ocean ridge lavas). The rest of the Sør-Varanger rocks in this paper define a trend with increasing La and U enrichment over Nb which can be interpreted as a result of addition of subduction component to their mantle sources. In modern subduction zone systems, this component can be represented by either fluid or silica-rich melt derived from downgoing slab and introduced into an overlying sub-arc mantle wedge to form a range of hybridized, subduction-modified mantle sources (Perfit et al., 1980; McCulloch & Gamble, 1991; Hawkesworth et al., 1994; Kepezhinskas et al., 1996; Pearce, 2008). In this scenario, various parts of the subducted slab, namely sediment, basaltic crust and upper mantle serpentinite or a mixture thereof, can contribute to the geochemical inventory of subduction-related, ultramafic-mafic magmas (Thirlwall et al.,

1996; Plank & Langmuir, 1998; Spandler & Pirard, 2013).

This subduction enrichment signature of ultramafic-mafic magmas in the Sør-Varanger area can be further emphasized by co-variation of La/Nb and Ba/Nb (Fig. 12). Again, a number of Sør-Varanger ultramafic-mafic rocks are grouped around the low La/Nb and Ba/Nb values typical of oceanic magmas while the rest of the compositions define two distinct trends with more or less

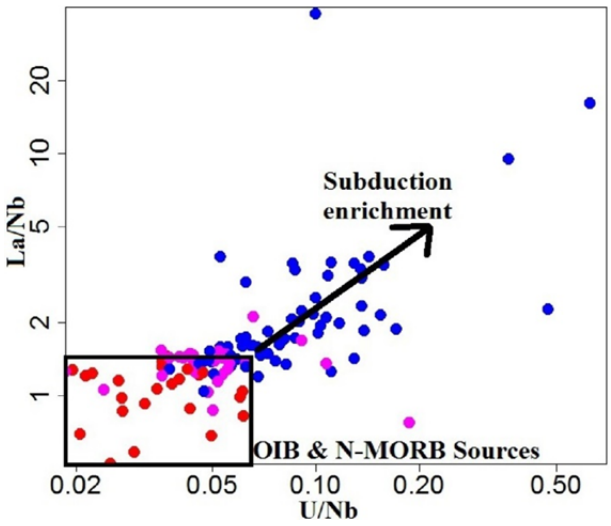

Figure 11. La/Nb versus U/Nb graph for ultramafic-mafic rocks from the Sør-Varanger area

Note. La-U-Nb ratios defining the OIB and N-MORB mantle sources are from Niu & O'Hara (2003).

simultaneous increase in both La/Nb and Ba/Nb ratios and with distinct Ba enrichment over Nb coupled with the lack of similar LREE/HFSE enrichment (Fig. 12). The La-Ba enrichment trend is best interpreted as an addition of subducted sediment component to the source region (Avanzinelli et al., 2009; Conticelli et al., 2009) while the Ba enrichment without well-defined LREE enrichment can be possibly caused by assimilation of volcanic arc crust in an active subduction setting (Kay, 1980; Chiaradia et al., 2009).

Geochemical variations in ultramafic-mafic rocks from Sør-Varanger area (Arctic Norway) indicate that their parental melts were derived from multiple mantle sources. Some of the rocks exhibit trace element characteristics typical of depleted (N-MORB) to enriched (E-MORB and OIB) oceanic mantle. This lithospheric heterogeneity may possibly reflect early mantle differentiation processes which are now well-documented for both Hadean and Archean time (Blichert Toft & Albarede, 1994; Frei et al., 2004; Carlson & Boyet, 2008; Shirey et al., 2008; Hoffmann et al., 2010; Polat et al., 2011; Dhuime et al., 2012). It is possible that Hadean to Archean mantle differentiation lead to the formation of multiple lithospheric sources beneath the Norwegian Craton which later gave birth to the entire range of ultramafic-mafic rocks documented within the Sør-Varanger area.

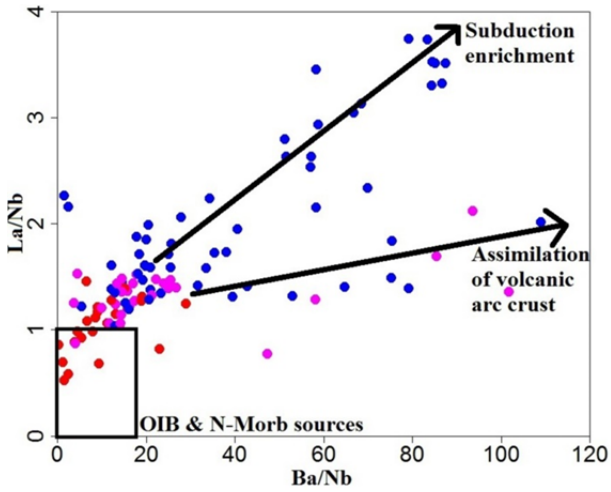

Figure 12. La/Nb versus Ba/Nb graph for ultramafic-mafic rocks from the Sør-Varanger area

Note. La-Ba-Nb ratos defining the OIB and N-MORB mantle sources are from Niu & O'Hara (2003).

Alternatively, lithospheric mantle beneath the Norwegian craton could have inherited this mantle source heterogeneity from earlier cratonic terranes that were assembled (accreted) together during Eoarchean to Mesoarchean to form a proto-Fennoscandian shield. Some of these proto-cratonic Eoarchean crustal ages are still preserved in felsic gneisses from Sør-Varanger area (3.69 Ga; Kepezhinskas, 2011a) and reflect crustal processes that took place prior to amalgamation of the Norwegian craton itself (within the general ramifications of tectonic model proposed by Nutman et al. (2015)). Such craton amalgamation possibly involved various incipient oceanic and subduction-related processes which may or may not be directly correspondent to the plate tectonic processes operating in modern (Phanerozoic) Earth. These processes include, but are not limited to, subduction zone and collisional magmatism, plume head tectonics, collision of oceanic plateaus with subduction zones, ridge-trench tectonics as well as various modes of incorporation of the ocean plate stratigraphy (OPS) into ancient accretionary orogens (Kusky & Polat, 1999; Puchtel et al., 1999; Polat et al., 2002; Wyman et al., 2002; Smithies et al., 2005; Jenner et al., 2009; Manikyamba et al., 2008; Manikyamba et al., 2009; Mueller et al., 2010; Szilas et al., 2012b; Bedard et al., 2013; Kusky et al., 2013; Furnes et al., 2015). Under this multistage scenario, komatiites (as presented above in this study) and banded iron formation (BIF) rocks cropping out near Kirkenes and Bjornevatn (Melezhik & Sturt, 1994) were probably formed within an Archean accretionary setting not unlike the Central Orogenic Belt in North China Craton (Wang et al., 2013; Kusky et al., 2013), Archean accretionary belts (Abitibi, Wawa, Superior) of the Canadian Shield (Kerrich et al., 1998; Wyman, 1999; Polat & Kerrich, 2001; Polat & Kerrich, 2002; Polat & Munker, 2004; Canil, 2008) as well as the Archean greenstone terranes of the Baltic Shield (Puchtel et al., 1999). Melting of this heterogeneous lithospheric mantle followed by polybaric crystal fractionation and possibly some limited assimilation of subduction-modified crust (volcanic arc crust trend in Figure 11) produced a range of primary ultramafic-mafic magmas in the Norwegian Arctic from komatiites and komatiitic basalts through various tholeiitic and alkaline basalts to shoshonitic lamprophyres.

5.2 Possible Tectonic Interpretation of Sør-Varanger Shoshonitic Lamprophyres

Tectonic interpretation of shoshonite volcanic rock series has been a subject of debate for over last 40 years. Early publications on the subject recognized that shoshonites – along with high-K calc-alkaline rocks – are integral part of convergent margin magmatism and are produced by melting of island-arc mantle at deeper depths beneath an island-arc system compared to the tholeiitic and calc-alkaline volcanics (Joplin, 1968; Jolly, 1971; Keller, 1974; Morrison, 1980). Later experimental and geochemical modelling of shoshonite petrogenesis suggested that these K-rich melts are probably formed by partial melting of hydrated mantle source fluxed by LILE-rich fluid component derived from a subducting slab which later undergo moderate- to low-pressure fractionation of clinopyroxene-amphibole-plagioclase assemblages to form differentiated (absarokite-shoshonite-banakite-latite) shoshonites series (Pe Piper, 1980; Pe Piper, 1983; Kontak et al., 1986; Meen, 1989; Sun & Stern, 2001; Leslier et al., 2009). It was also established that shoshonite series occur in a variety of tectonic settings that include oceanic arcs such as Marianas and Fiji (Stern et al., 1988; Gill & Whelan, 1989; Sun & Stern, 2001; Leslie et al., 2009), mature convergent margins such as Andes and Kamchatka (Kontak et al., 1986; Kepezhinskas, 1994) as well as a various collisional orogens at different stages of their evolution

such as Alps, Tianshan, Tibet (Sloman, 1989; Aitchinson et al., 2007; Conticelli et al., 2009; Yang et al., 2012). It was also suggested that small volume of shoshonite magmas in convergent margin environments as opposed to calc-alkaline rocks and arc tholeiites may have resulted from low-degree decompression melting of variably enriched (by slab fluid component) sub-arc mantle wedge as opposed to large-degree melting of water-fluxed mantle wedge to produce calc-akaline magmas that dominate Paleozoic to modern island arcs and continental margins (Leslier et al., 2009). Archean shoshonites described in several cratonic terranes in Canada display geochemical characteristics similar to modern shoshonites and are interpreted as low-degree melts from an enriched source in an Archean convergent margin tectonic setting (Brooks et al., 1982; Dostal & Mueller, 1992; Wyman & Kerrich, 1993).

Based on all this work and utilizing an extensive chemical database of shoshonite rocks worldwide, Kepezhinskas (1994) demonstrated that shoshonite rock series can be in principal divided into two geochemical sub-groups on the basis of TiO_2-K_2O-SiO_2 relationships: low-Ti and high-Ti shoshonites (Fig. 9). Low-Ti sub-group includes most rocks from the oceanic arcs and continental margins that were formed mostly within compressional tectonic regime due to ocean-ocean or ocean-continent subduction (Kepezhinskas, 1994). High-Ti group encompasses a range of extensional regimes related either to intra-arc, behind-the-arc or back-arc extension, oceanic arc rift propagation or syn-collisional and post-collisional rifting of compressional orogens (Kepezhinskas, 1994; Conticelli et al., 2009; Leslie et al., 2009; Ishizuka et al., 2010). Nethetheless, both geochemical groups of shoshonite volcanic series are associated with convergent margin tectonic settings and can be used as paleotectonic indicators of these geodynamic environments in the geological past.

As we have shown above, shoshonitic lamprophyres from the Sør-Varanger area fall into both sub-groups on the TiO_2-SiO_2 and TiO_2-K_2O discrimination plots (Fig. 9). This geochemical classification corresponds well with diverse trace element characteristics of Sør-Varanger shoshonitic lamprophyres described in the geochemical section above. High-Ti shoshonites have slightly depleted to undepleted primitive mantle-normalized compositions, while low-Ti (volcanic arc) shoshonites are always characterized by well-defined negative Nb and Ta anomalies (Meen, 1989; Kepezhinskas, 1994; Sun & Stern, 2001). Shoshonitic lamprophyres from Sør-Varanger exhibit enriched REE patterns coupled with well-defined negative Sr anomaly (Fig. 8B) which are consistent with derivation of parental shoshonite melts from subduction-fluxed sub-arc mantle wedge and their subsequent crystal fractionation via removal of plagioclase-rich assemblages at upper mantle to lower and mid-crustal levels (Meen, 1989). This interpretation is supported by common occurrence of large, chemically resorbed plagioclase phenocrysts (megacrysts?) in Sør-Varanger shoshonitic lamprophyres (Tab. 1) suggesting early removal of calcic plagioclase (negative Sr-anomalies on primitive mantle-normalized patterns; Fig. 8B) from high-pressure shoshonitic magma. It is important to emphasize here that the early fractionation of plagioclase (probably along with Ti-magnetite, amphibole and clinopyroxene; Pe Piper, 1983; Meen, 1989) has resulted only in formation of a differentiated suite of shoshonitic rocks (ranging from Mg-absarokite to evolved shoshonite compositions) but was not capable of generating of two types – high-Ti and low-Ti – of shoshonitic magma as observed in dikes and sills in the Sør-Varanger area. These two chemical sub-types of shoshonite rocks series were most probably created from different mantle sources and under somewhat different geodynamic conditions.

Unfortunately at this stage we can only demonstrate presence of both low-Ti and high-Ti shoshonites in the Sør-Varanger area and propose that these potassic rocks were formed in a range of convergent margin settings. Since no geochronological data yet exist for these rocks and no field relationships (such as cross-cutting relationships) are available from our field mapping efforts over last 7 years, we can only suggest that shoshonite magmas were generated via partial melting of variably enriched mantle sources and emplaced into Archean terranes within a convergent margin environment. Further investigation of these interesting rocks is certainly highly warranted especially taking into account that some shoshonitic lamprophyres in Sør-Varanger contain microdiamonds.

5.3 Presence of "Subduction" Geochemical Signature and Possible Role of Convergent Margin Processes in the Formation of Sør-Varanger Rocks

Current paradigm in the earth sciences suggests that true plate tectonics (comparable to modern day plate tectonic style) and hence, subduction as a process, started to operate in full capacity only in Neoproterozoic following a major geologic reformation that our planet went through at the Archean-Proterozoic boundary (Condie & Kroner, 2013). Although this view is supported by a widespread occurrence of ophiolites, bluschists and ultrahigh-pressure rocks that appear on the massive scale in Neoproterozoic (Stern, 2002). One of key tectonic indicators of the Wilson cycle are ophiolitic assemblages which represent fragments of the ancient oceanic lithosphere tectonically incorporated into accretionary structure of Phanerozoic mobile belts as well as

Precambrian cratons.

Ophiolites *sensu stricto* were initially defined at the 1972 Penrose conference and by Coleman (1971) and Moores & Vine (1971) as a "distinctive assemblage of mafic to ultramafic rocks that includes, from bottom to top, tectonized peridotites, cumulate peridotites, and pyroxenites overlain by layered gabbros, sheeted basaltic dikes, a volcanic sequence, and a sedimentary cover; an ophiolite may be incomplete, tectonically dismembered, or metamorphosed" (Dilek & Furnes, 2011). Almost immediately, it was recognized by Miyashiro (1975) that some ophiolites differ from the classic (in the Penrose Conference sense) oceanic crustal model and might have been formed in an island arc setting. Numerous studies that followed this groundbreaking work established the fact that ophiolitic rock assemblages as originally defined – sediments, pillow basalts, sheeted dikes, gabbros and mantle peridotites – could have formed in a wide range of oceanic and subduction environments that include a mid-ocean ridge itself, a transform-fault domain, and a set of supra-subduction zone settings such as a fore-arc, an island arc and a back-arc basin (Dilek & Furnes, 2011). Several attempts were made to classify ophiolites into a lherzolitic (roughly oceanic) and harzburgitic (roughly supra-subduction) type based on a chemistry of mantle peridotite section (Boudier & Nicolas, 1985), a high-Ti (roughly oceanic) and a low-Ti (roughly subduction-related) types based on a chemistry of gabbroic unit (Serri, 1981) and a Tethyan (Mediterranean) and Cordilleran (Circum-Pacific) types on the basis of their relative mode of tectonic emplacement (Beccaluva et al., 2004). Currently, a general approach appears to suggest that an ophiolitic ocean crust assemblage could have been formed in two main groups of tectonic environments – general oceanic and general supra-subduction (Dilek & Furnes, 2011). But in any case, tectonically dismembered, fragmented, partial and/or metamorphosed ophilite assemblages are widely accepted to represent various stages of Wilson cycle preserved in Precambrian and Phanerozoic geologic record (Pearce, 2008; Dilek & Furnes, 2011; Furnes et al., 2015).

Are there any other geologic indicators (specific rock associations, geologic structures, etc.) that can be used to decipher the paleotectonic environments that existed during amalgamation of the Norwegian Craton? For the purpose of this discussion, we will consider the following rock associations as recognized indicators of a convergent margin environment: 1) low-Ti (subduction-related) shoshonitic suites derived from a subduction-modified sub-arc mantle (see Kepezhinskas, 1994 for classification of shoshonites into a low-Ti and high-Ti chemical groups; Thompson & Fowler, 1986; Manikuyamba et al., 2012); 2) boninites which reflect specific melting conditions in a highly depleted mantle wedge (Cameron et al., 1983; Beccaluva & Serri, 1988; Polat et al., 2002; Konig et al., 2010); 3) eclogites (including retrograded) which mark UHP metamorphic conditions consistent with common subduction processes (Mints et al., 2010; Tappe et al., 2011a); 4) low-Ti basalts with "subduction" geochemical signatures and differentiated (basalt to rhyolite) calc-alkaline volcanic series which are commonly viewed as petrogenetic indicators of convergent margin processes (Myashiro, 1974; Perfit et al., 1980; Hawkesworth et al., 1994; Mueller et al., 2010) and 5) Nb-enriched arc basalts (NEABs) which reflect a unique interaction of slab-derived adakitic melts with mantle wedge peridotite in a variety of subduction regimes (Kepezhinskas et al., 1996, Sajona et al., 1996; Hastie et al., 2011).

As presented in this paper, some ultramafic-mafic rocks in the Sør-Varanger area exhibit geochemical characteristics – primarily depletions in HFS elements such as Ti, Nb and Ta – which could have been formed via addition of LILE-enriched fluid to a variably enriched mantle within a convergent margin environment. To test the hypothesis that at least some mantle sources in the Sør-Varanger area may have experienced addition of an enriched fluid component, we plotted our ultramafic-mafic rocks on the Th/Yb-Nb/Yb graph of Pierce (2008). On this geochemical diagram (Fig. 13), Sør-Varanger rocks form a continuous compositional array located slightly above and parallel to the MORB-OIB array defined by recent mid-ocean ridge and ocean island basalts (Pearce, 2008). Two analyses of magnesian basalts and one shoshonitic lamprophyre form an oblique trend towards higher Th/Yb and Th/Nb ratios (Fig. 13). This trend can be interpreted in several ways: it can represent the AFC evolution of at least some primitive basalts and shoshonites in Sør-Varanger, manifest crustal recycling (for example, via addition of a sediment melt or fluid component in a convergent margin environment), or record contamination by a small amount of volcanic arc or continental crust of mantle-derived melts (Pierce, 2008). Position of Sør-Varanger rocks slightly above and parallel to the mantle MORB-OIB mantle array at higher Th/Nb ratios may indeed indicate an addition of small amounts of "subduction" component to variably enriched mantle sources beneath the Sør-Varanger area as emphasized by Th/Yb-Nb/Yb variations (Fig. 13). If this is correct, we can propose that convergent margin processes may have played an important role in the formation and evolution of the Norwegian cratonic terranes.

This is further confirmed by the Zr/Nb-Nb/Th relationships illustrated in Figure 14. Ultramafic-mafic rocks plot into the fields of hydrated and enriched mantle (HM and EM, respectively, Figure 14) and form a continuous compositional array from high Zr/Nb and low Nb/Th to low Zr/Nb and high Nb/Th values (Fig. 14). Hydrated

mantle field in Figure 14 indicated magma formation in a variety of arc, backarc and forearc settings by hydrous melting of a variably depleted mantle wedge source (Condie, 2015). Enriched mantle field encompasses oceanic plateau and island basalts and assocated rocks most likely produced by decompression melting of a mantle plume source in a plume or crustal delamination environment (Condie, 2015). Presence of "hydrated mantle" geochemical characteristics in some Sør-Varanger rocks supports involvement of convergent margin processes in petrogenesis of ultramafic-mafic magmas in the Norwegian Arctic.

We propose in this paper (Fig. 15) that this convergent margin environment might have been formed during interaction of Archean cratonic terranes with the Belomorian-Lapland Ocean Basin (BLOB in Fig. 15). Oceanic lithosphere formed within BLOB spreading center was either subducted or subcreted (possibly along with gravitational delamination of basaltic crust) along the Archean margins of the Norwegian craton in the north and Karelian craton in the south (Fig. 15). Relics of this basaltic crust may be represented by 2.87 Ga MORB-type eclogites within the Belomorian suture zone (Mints et al., 2010; Balagansky et al., 2014). Subduction or subcretion of Archean oceanic crust progressively led to release of water-rich fluids from the uppermost oceanic crust and pelagic (mostly pelitic, Al-rich) sediment that fluxed the depleted mantle (DM in Figure 12) of the sub-arc wedge and enriched it with incompatible elements (such as Ba, Th, U, LREE).

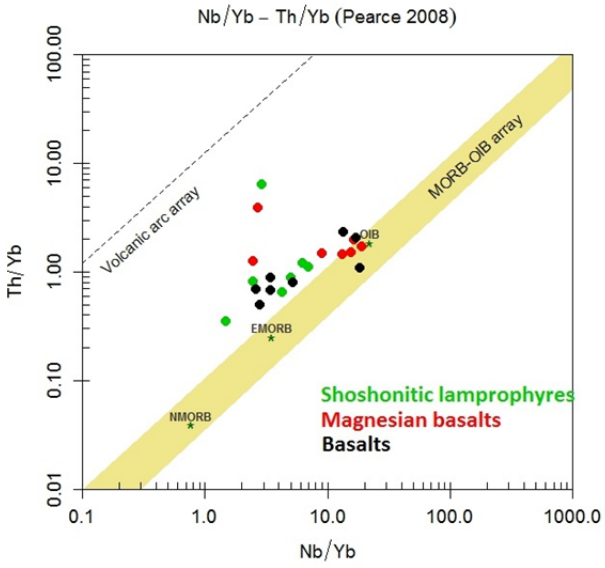

Figure 13. Shoshonic lamprophyres, magnesian basalts and basalts from the Sør-Varanger area plotted on the Th/Yb-Nb/Yb discrimination diagram of Pierce (2008)

Melting of this "subduction"-modified (we use the term "subduction" here rather loosely referring only to a hydrous fluid enriched in LILE and LREE) source (EM1) created various HFSE-depleted magmas such as shoshonitic lamprophyres, magnesian basalts and subduction-related basalts described in this study. We also suggest that enriched (within plate-type) mafic magmas that are also present among the products of ultramafic-mafic magmatism in the Norwegian Lapland could have been generated by adiabatic melting of the within-plate (OIB-type) mantle source (EM2; Fig. 12) that ascended into the mantle wedge beneath an Archean convergent margin possibly through structural discontinuities in the delaminated basaltic crust roughly following the model of Morris & Hart (1983). These processes of interaction between delaminated basaltic crust and Archean terranes that form the Norwegian craton eventually led to a variety of mantle sources that are documented in ultramafic-mafic rocks from the Sør-Varanger area.

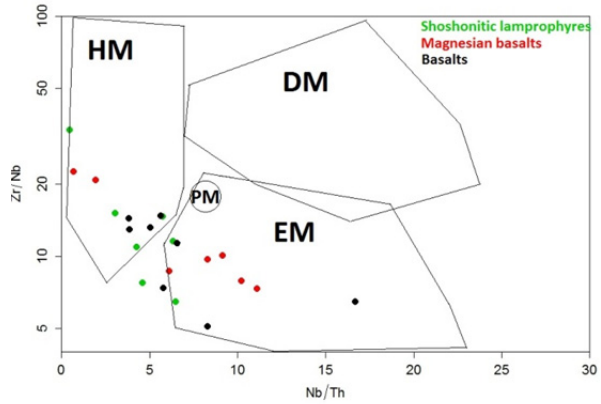

Figure 14. Shoshonic lamprophyres, magnesian basalts and basalts from the Sør-Varanger area plotted on the Zr/Nb-Nb/Th discrimination diagram

Note. Fields of hydrated mantle (HM), enriched mantle (EM) and depleted mantle (DM) are after Condie (2015).

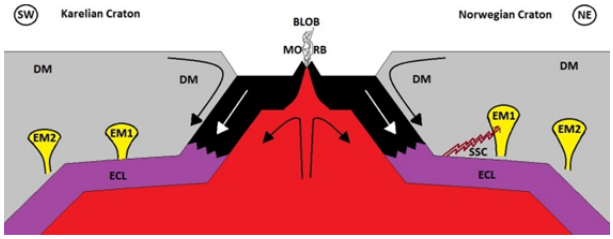

Figure 15. A simplified cartoon illustrating the proposed tectonic setting for a development of Archean mantle heterogeneity responsible for the generation of the Eastern Finnmark ultramafic-mafic magmas

Note. BLOB- Belomorian-Lapland Ocean Basin, ECL-eclogite, SSC-subducted sediment component, DM-depleted mantle, EM1-enriched lithospheric mantle re-fertilized by slab sediment-derived melts, EM2-enriched within-plate mantle.

The Norwegian craton shares at least three fundamental geologic characteristics with diamond-bearing cratons around the world: 1) thick (at least in excess of 45 km) continental crust; 2) Archean (3.69-2.5 Ga) age of its crustal rocks and 3) low heat flow (Artemieva, 2003). These common properties suggest that the lithospheric mantle beneath Eastern Finnmark can potentially contain diamonds. Presence of ultramafic-mafic rocks generated under mantle conditions from geochemically heterogeneous sources – especially such rocks as shoshonitic lamprophyres – indicate that local conditions might have existed to allow some of these mantle-derived magmas to assist diamond transport to the surface through major shear zones in the Norwegian cratonic lithosphere. In the section below, we attempt to briefly evaluate a potential for the existence of diamond among Archean crustal complexes of the Norwegian craton.

5.4 Some Implications for Diamond Exploration in the Norwegian Lapland

Archean cratons are among the few geologic terms that have a familiar buzz for people from both the main street – university professors and geology aficionados – and from the Wall Street such as investment fund managers and MBA-graced mining analysts. The common link has a simple but alluring name and is called diamond. Diamond is a compacted form of carbon produced at great pressures deep inside Earth and is known to mankind from the old age of the Golkonda mines in ancient India. Diamonds are incrusted into Maharajas scepters, crowns of mighty rulers and diadems of their queens of an unparalleled beauty. Diamonds seem to be both eternal and ethereal and certainly are one of the best candidates to be a Girl's best friend.

Diamonds are being brought to the surface by some fast moving volcanic rocks such as kimberlites and lamproites which, with some minor exceptions, are restricted to the inner cores of the ancient hearts of our continents – cratons (Shirey et al., 2004; Stachel & Harris, 2008; Kjarsgaard, 2007). Most of highly profitable

and prolific diamond mines – including famous South African, Siberian and Canadian diamond fields – are located within Archean cratonic terranes (Kjarsgaard, 2007; Gurney et al., 2010). Additional mantle-derived magmas that can potentially carry diamonds to the surface include various ultramafic to mafic lamprophyres and water-rich (presence of phlogopite and/or amphibole in case of Sør-Varanger komatiites) komatiitic melts (Tables 6, 7 and 8; Kaminsky, 2007). Some new models of diamond formation are centered on the introduction of sedimentary carbon via shallow Archean subduction and formation of diamonds in the sub-arc mantle wedge and subducted slab rather than the deep roots of Archean cratons associated with traditional diamond deposits (Shirey et al., 2004; Wyman et al., 2006; Shirey & Richardson, 2011). This is now supported by a plethora of new mineralogical (presence of Mg-Al-Si-rich mineral phases, Ca-carbonates and graphite as diamond inclusions) and geochemical (Re-Os isotopic signatures in sulfide diamond inclusions, crustal C-N compositions of diamonds, presence of K-Na-Cl-H_2O-rich fluids and Ba-U-Th-LREE enrichment coupled with Nb-Ta depletions in high density fluid inclusions in diamonds) data suggesting large-scale participation of slab-derived fluids and remnant slabs (eclogites) at least in some Archean cratonic environments (Richardson et al., 2001; Westerlund et al., 2006; Shirey & Richardson, 2011; Loginova et al., 2015; Weiss et al., 2015; Shu et al., 2016). Hybridization of Archean cratonic mantle by slab-derived, water-rich siliceous fluids is also well documented in some harzburgitic xenoliths from diamond-bearing kimberlites in South Africa (Bell et al., 2005).

Table 6. Examples of tectonic and petrologic interpretation of diamond-bearing lamprophyric rock series

Geographic location	Tectonic setting/Geologic interpretation	Petrologic interpretation	References
Torngat and Abloviak lamprophyric intrusions, North Labrador and Quebec, Canada	Rifting of the Paleoproterozoic suture zone within the Archean North Atlantic craton	Melting of the ancient MARID-type veined lithospheric mantle metasomatized by CO_2-rich potassic silicate melt	Digonnet et al., 2000; Tappe et al., 2008
Renard igneous bodies, Otish Mountains, Quebec, Canada	Transition from active margin environment to initial rifting associated with opening of the Iapetus ocean	Melting of garnet-bearing lithospheric mantle source	Birkett et al., 2004
Akluilak dikes, Nunavut province, Canada	Rifting of the central Churchill province	Melting of deep lithospheric mantle source	MacRae et al., 1995
Killala spessartite lamprophyre dike, Marathon area, Ontario, Canada	Trans-Superior Tectonic Zone (suture) within the Archean Superior craton	Melting of enriched mantle source	Platt & Mitchell, 1982
Kyle Lake pipes, James Bay Lowlands, northern Ontario	Rifting of the Archean Superior craton	Ultramafic lamprophyric magma contaminated granitic gneiss	Kaminsky, 2007
Wawa lamprophyric breccias, pipes and dikes, Ontario, Canada	Michipicoten greenstone belt (2.66-2.73 Ga), essentially an ancient active margin analogue of Western Mexican arc	Subduction-induced melting of lithospheric mantle source	Wyman et al., 2006
Sarfartoq aillikites, West Greenland	Proterozoic mobile belt in West Greenland	Melting of a deep (sub-lithospheric) subduction-modified source; melting of North Atlantic mantle modified by asthenosphere-derived carbonate-rich melt	Nielsen et al., 2009; Tappe et al., 2011
Nepheline monchiquite pipes and dikes, Onega Peninsula Arkhangelsk province, NW Russia	Neoproterozoic rifting of the Archean Kuloi craton	Melting of lithospheric, garnet-bearing mantle source	Kaminsky, 2007
Mhadjgawat and Panna pipes and dikes, India	Mesoproterozoic rifting of the Archean Dharwar craton	Melting of enriched mantle source metasomatized by ancient subduction component (sediment?)	Chalapathi Rao, 2005; Chalapathi Rao et al., 2013
Karashoho	Hercynian Tyan-Shan	Melting of lithospheric	Golovko &

picrite-shoshonite-absarokite pipe, Uzbekistan	orogeny separating Precambrian Kyzylkum and Syr-Daria microcontinents or cratonic terranes	metasomatized (subduction-related?) mantle source followed by crustal contamination	Kaminsky, 2010

The Norwegian craton – as all the other cratonic terranes – is associated with an Archean age (3.7-2.5 Ga), thick continental crust (45-55 km) and low heat flow (Artemieva, 2003; Artemieva, 2007; Kepezhinskas, 2011a). Diamonds in Norway were first discovered by C. Rabot in 1887 in peculiar, red-colored sediments ("purple sands") in the Pasvik river valley and confirmed as diamonds by C. Velain who at the time was the distinguished professor of mineralogy at the Museum of Mineralogy in Paris, France. Oslo-based Kimberlitt AS began its quest to identify commercial diamond deposits in the Norwegian Lapland in 2009 and since this inception date achieved substantial progress in diamond exploration around the commune of Sør-Varanger. Systematic sampling of Quaternary till, lake and stream sediment revealed presence of a range of kimberlite indicator minerals (Kepezhinskas, 2011a; Kepezhinskas, 2011b). Kimberlite indicator minerals are typically regarded as phases that were formed together with diamond within its stability window in the cratonic lithosphere (Kjarsgaard, 2007). They are more abundant than diamond and are generally easier to locate. Kimberlite indicator minerals discovered in the Sør-Varanger area include Mg-rich olivine, chromite, chrome diopside as well as some "exotic" diamond indicator minerals such as corundum and Ca-rich garnet (uvarovite; Kepezhinskas, 2011b). Discovery of corundum and uvarovite is especially important in the context of the data and interpretations presented above since both mineral phases are linked to ancient subduction of carbonate and pelitic (Al-rich) sediment beneath Archean cratons. Most indicator minerals show only limited degrees of chemical abrasion indicating their derivation from local magmatic sources. It is important to emphasize that chemistry of some indicator minerals such as chrome diopside and chromite supports their derivation from the stability field of diamond in the mantle which suggests presence of diamond within the Norwegian craton (Kepezhinskas, 2011a; Kepezhinskas, 2011b).

Table 7. Average chemical compositions of komatiites and shoshonitic lamprophyres from Sør-Varanger (SV) compared to some diamondiferous ultramafic-mafic rocks in Precambrian and Phanerozoic tectonic environments

	SV komatiites	SV shoshonitic lampro-phyre	Dachine komatiite Guiana[(1)]	Olondo ultramafic schist, Aldan shield, Siberia[(2)]	Wawa calc-alkaline lampro-phyre[(3)]	Khaderpet pipe, India[(4)]	Shoshonitic lamprophyre, Sikhote-Alin Orogenic Belt[(5)]	Shoshonitic lampro-phyre, Uzbekistan[(6)]	Absarokite-picrite, Uzbekistan[(6)]
	N= 6	N= 7	N= 9	N= 1	N= 4	N= 5	N= 2	N = 17	N = 11
SiO_2	44.97	49.27	43.5	37.9	47.60	40.12	41.56	51.58	46.20
TiO_2	0.37	1.15	0.67	0.01	1.01	0.64	1.94	0.91	0.66
Al_2O_3	7.24	10.77	6.83	0.24	11.76	8.66	9.21	10.63	7.06
Cr_2O_3	0.487	0.007							
Fe_2O_3	11.62	13.11	11.12	5.9	11.34	4.136	5.92	7.65	8.09
MnO	0.17	0.17	0.12	0.06	0.15	0.16	0.16	0.15	0.11
MgO	25.08	12.39	20.9	36.6	13.64	13.5	13.95	8.49	18.17
CaO	5.89	6.36	4.80	0.07	8.12	10.70	12.73	7.97	6.46
Na_2O	0.80	0.64	0.83	0.44	2.22	0.73	1.76	1.88	1.05
K_2O	0.20	3.33	0.61		3.35	1.09	1.54	4.92	2.81
P_2O_5	0.04	0.16	0.23	0.15	0.37	0.22	0.265	0.40	0.18
LOI	3.63	2.31	10.00	18.6		9.8	3.96	4.69	7.89
Total	100.32	99.7	99.6	100*		89.786	92.98	99.27	98.68
Ni	1043.12	180.89	850		423		246.67	235	545
Co	91.1	60.1			53	54.8	49.77	49	54
V	141.5	273.9			211	84.6	182.3	256	131
Ba	81	501	146		831	291	174.58	1783	56
Sr	83.9	96.0	236		362	282.4	262.82	458	215
Rb	5.7	148.4	22.8		96	40.1	39.62	146	109

Cs	0.4	5.7	2.41		4.3		13.65		
Zr	30.2	80.6	47		80	91	135.84	295	97
Y	7.6	18.6	11.3		18.3	11.6	14.1	41	13
Nb	1.5	7.3	3.89		3.7	35.9	24.7	30	ND
Ta		0.65			0.24	1.7	1.5	6.3	ND
Hf	0.8	2.4			2.3	0.13	3.33		
Th	0.5	1.7	0.56		2.5	14.9	1.8	13.9	3.5
U	0.1	0.6			0.7	5.1	0.5	6.0	2.9
La	4.2	12.9	6.62	0.57	16.8	51.6	19.1	49.7	11.0
Ce	8.7	32.3	15.92	1.19	39.1	94.7	40.5	97.9	28.3
Pr	1.11	4.3		0.14	5.6	11.5	3.6		
Nd	5.0	18.8	9.41	0.53	24.7	39.5	21.7		
Sm	1.09	3.91	2.25	0.12	5.6	27.03	4.65	2.25	3.60
Eu	0.35	1.08	0.62	0.03	1.8	1.48	1.38	2.80	0.89
Gd	1.21	3.77	2.04	0.1	5.0	3.9	4.08	9.60	2.67
Tb	0.20	0.61		0.01	0.7	0.44	0.61	1.97	0.59
Dy	1.30	3.48	1.94	0.07	3.5	2.32	3.30	5.10	2.94
Ho	0.27	0.68		0.02	0.7	0.39	0.63		
Er	0.81	1.86	1.08	0.05	1.8	1.02	1.51		
Tm	0.12	0.28		0.01	0.3	0.14	0.21		
Yb	0.79	1.77	1.06	0.05	1.6	0.91	1.13	2.50	1.52
Lu	0.12	0.26	0.17	0.01	0.2	0.132	0.18	3.80	0.26

Note. Data sources: (1) Capdevilla et al. (1999); (2) Smelov et al. (2012); (3) Wyman et al. (2006); (4) Smith et al. (2013); (5) Ivanov et al. (2005); (6) Golovko & Kaminsky (2010). *Recalculated on anhydrous basis. ND – not detected.

Presence of corundum and Ca-rich garnet (uvarovite) is also quite significant since both minerals are commonly found in diamond-rich eclogite xenoliths in kimberlites (frequently with diamond grades in excess of 100 carats per ton) as well as in some high-grade kimberlites in Canada, Siberia and India.

Recent research suggests that all Archean cratons are not equal and some were assembled (accreted) in a different fashion compared to some classic cratonic environments such as South Africa and Siberia. These "other"cratons – best examples are probably North American cratons (Wyoming, Slave, Superior), cratons of NW Russia (Karelian, Kola and Kuloi notoriously known among diamond exploration geologists as "KKK" cratons) and Indian cratons (Dharwar and others) – are characterized by protracted history of crustal convergence marked by dismembered ophiolite assemblages, products of large-scale slab melting and mantle hybridization such as adakites and high-Nb basalts as well as various continental margin lavas such as low-Ti tholeiites, boninites and differentiated basalt-andesite-dacite-rhyolite series. These cratons host some spectacular and highly profitable diamond mines (Ekati, Diavik, Renard, Majhgawan, Grib and Lomonosov, to name a few) that produce substantial amounts of large and highly valued precious stones of exceptional quality (Kjarsgaard, 2007; Tab. 6; Tab. 8). Here we propose to call them "subduction-modified cratons" as opposed to "classic" cratons that for different reasons have not experienced the same amount of Archean subduction. It is important to emphasize that large scale subduction of Belomorian-Lapland Ocean Basin (BLOB) lithosphere beneath the Karelian craton most probably contributed to the formation of the commercial diamond deposits in Finland (Fig. 15). Judging from some obvious parallels in the Karelian and Norwegian cratons amalgamation, we have all reasons to expect that similar diamond mineralization is presented within the Sør-Varanger segment of the Norwegian craton.

All the data presented above suggest that the Norwegian craton can be classified as subduction-modified craton. Geologic and petrologic comparison of its crustal structure and rock associations with other subduction-modified cratons – such as Canada, India and NW Russia – reveals its high perspectivity in hosting commercial diamond deposits. However, only focused, concentrated and well-guided exploration efforts will allow us to unlock the hidden treasures of the ancient Lapland in Norwegian Arctic.

6. Conclusions

Ultramafic-mafic rocks from Sør-Varanger display a range of major and trace element compositions suggesting that some rocks (komatiites and certain magnesian basalts) might be related via fractional crystallization while other rocks (shoshonitic lamprophyres and various basalts) were most probably produced by partial melting of

diverse lithospheric mantle sources.

These rocks have originated from several lithospheric mantle compositions ranging from depleted (N-MORB-type sources) to primitive and enriched (E-MORB/OIB-type sources) and to convergent margin lithospheric sources.

This diversity of mantle sources in Eastern Finnmark can be interpreted as a result of co-existence of several type of mantle sources in the cratonic lithosphere beneath the Norwegian craton. Alternatively, it could have been created through a series of mantle depletion/enrichment events that affected an originally homogeneous cratonic mantle of Arctic Norway, most possibly during Archean time.

Subduction-related modification - manifested by LILE and LREE enrichment of mantle-derived ultramafic-mafic rocks in Sør-Varanger area – was generated through introduction of subducted sediment-derived fluid or melt to depleted lithospheric mantle source. Possibility of Archean subduction beneath Norwegian craton is indicated by an occurrence of fragments of tectonic mélange and dismembered ophiolitic peridotites in the area as well as widespread Mesoarchean tonalite-trondhjemite-granite (TTG) magmatism.

Subduction provides an efficient mechanism of introduction of large amount of carbon extracted from subducted sediment into the overlying mantle wedge. Thermal regime and shallow subduction angles characteristic of Archean subduction zones allows for diamond formation and stabilization at shallower depths (100-160 km; Wyman et al., 2006) compared to younger Proterozoic and Phanerozoic tectonic environments (200-250 km). In this model, both sub-arc mantle wedge (peridotitic or P-type diamonds) and subducted slab (eclogitic or E-type diamonds) serve as a source of diamond mineralization in subduction-modified cratonic lithosphere. These Archean diamonds can later be picked up by several types of subduction-related, mantle-derived magmas and transported to the surface to form high-grade commercial diamond deposits.

Table 8. Diamond deposits developed in spatial, temporal or genetic association with lamprophyric magmas

Deposit	Rock association	Diamond grade (cpht*)	Estimated reserves or resources	Additional notes
Renard deposit, Quebec, Canada(1)	Kimberlite, ultramafic lamprophyre	75.5	17,947,000 carats	Potential producer of "Special" large diamonds – stones of > 50 carats per every 100,000 carats of diamonds recovered
Majhgawan deposit, India(2)	Transitional kimberlite, orangeite, lamproite, ultramafic lamprophyre	5-30	Resource in excess of 500,000 carats; annual production of 40,000 carats	Largest stone recovered - 28.25 carats, 42% of diamond population are gem-quality
Leadbetter deposit, Ontario, Canada(3)	Calc-alkaline volcaniclastic lamprophyre	35-71 average, enriched bands grading 214-264	Resource in excess of 3,000,000 carats	Mostly colorless octahedral diamonds
Karashoho deposit, Uzbekistan(4)	Shoshonitic lamprophyre, absarokite, picrite	0.87 to 2.55	Unknown resource	Diamond population dominated by colorless octahedral stones

Note. (1) Stornoway Diamonds website (www.stornowaydiamonds.com); (2) Chalapathi Rao (2005); (3) Dianor Resources website (www.dianor.com); (4) Golovko & Kaminsky (2010). * - carats per hundred tons.

Acknowledgements

The authors acknowledge continuous support and generous help from Kimberlitt AS (Oslo, Norway), especially that of the Company's Chairman Mr. Rune Rinnan. Numerous discussions with Tore Birkeland, Jørn Christensen, Kjell Trommestad, Morten Often, Hugh O'Brien, Marja Lehtonen, Jukka Marmo, Mark Collins and Rod Baker have been extremely encouraging and are gratefully acknowledged. Comments by Dr. Jean Bedard on the earlier version of this manuscript are greatly appreciated. We acknowledge unconditional help, support and companionship of our friends and colleagues in the field: Emil Danielsen Husby, Mick Hugo Eriksen, Bendik Lunde, Vårin Trælvik Eilertsen, Leslie Suen, Kjell Svindland, Mads Trulssen, Julia Sen, Arne Alnes, Valentine de Mercey, Elin Hviding Roalkvam, Ségolène Rabin, Christian Haugen Svendsen, Karl Masson, Matthieu Cedou,

Diego Martinez, Sandra Puig Rodes, Daniel Persen, Ingunn Hernes, Karina Gjerde, Kristoffer Walsh, Ane Damberg, Audun Sommerseth, Rebekka Dischington, Kurtis Christensen. P.K. wants to acknowledge a life-long discussion on the nature of the oceanic lithosphere and role of subduction processes through geologic time with the late Professor Nikita Bogdanov who was not only a forgiving supervisor and patient advisor but also a wise and unforgettable mentor and friend.

References

Adam, J., Rushmer, T., O'Neill, J., & Francis, D. (2013). Hadean greenstones from the Nuvvuagittuq fold belt and the origin of the Earth's early continental crust. *Geology, 40*, 363-366. http://dx.doi.org/10.1130/G32623.1

Aitchinson, J. C., McDermid, I. M. C., Ali, J. R., Davis, A. M., & Zyabrev, S. V. (2007). Shoshonites in Southern Tibet record Late Jurassic rifting of a Tethyan intraoceanic island arc. *Journal of Geology, 115*, 197-213. http://dx.doi.org/10.1086/510642

Allegre, C. J. (1982). Genesis of Archaean komatiites in a wet ultramafic subducted plate. In N.T. Arndt & E.G. Nisbet, E. G. (Eds.). *Komatiites* (pp. 495-500). London: George Allen and Unwin.

Anderson, D. L. (2005). Large igneous provinces, delamination, and fertile mantle. *Elements, 1*, 271-275. http://dx.doi.org/10.2113/gselements.1.5.271

Artemieva, I. M. (2003). Lithospheric structure, composition, and thermal regime of the East European Craton: implications for the subsidence of the Russian Platform. *Earth and Planetary Science Letters, 213*, 429-444. http://dx.doi.org/10.1016/S0012-821X(03)00327-3

Artemieva, I. M. (2007). Dynamic topography of the East European Craton: shedding light upon lithospheric structure, composition, and mantle dynamics. *Global and Planetary Change, 58*, 411-434. http://dx.doi.org/10.1016/j.gloplacha.2007.02.013

Artemieva, I. M., & Thybo, H. (2008). Deep Norden: highlights of the lithospheric structure of Northern Europe, Iceland, and Greenland. *Episodes, 31*, 98-106.

Avanzinelli, R., Lustrino, M., Mattei, M., Melluso, L., & Conticelli, S. (2009). Potassic and ultra-potassic magmatism in the circum-Tyrrhenian region: significance of carbonated pelitic vs. pelitic sediment recycling at destructive plate margins. *Lithos, 113*, 213-227. http://dx.doi.org/10.1016/j.lithos.2009.03.029

Azbel, I. Ya, Buyanov, A. F., Ionkis, V. T., Sharov, N. V., & Sharova, V. P. (1989). Crustal structure of the Kola Peninsula from inversion of deep seismic sounding data. *Tectonophysics, 162*, 87-99. http://dx.doi.org/10.106/0040-1951(89)90357-0

Balagansky, V., Shchipansky, A., Slabunov, A. I., Gorbunov, I., Mudruk, S., Sidorov, M., … Voloshin, A. (2014). Archaean Kuru-Vaara eclogites in the northern Belomorian Province, Fennoscandian Shield: crustal architechture, timing, and tectonic implications. *International Geology Review, 57*, http://dx.doi.org/10.1080/00206814.2014.958578

Barnes, S. J., & Often, M. (1990). Ti-rich komatiites from northern Norway. *Contributions to Mineralogy and Petrology, 105*, 42-54. http://dx.doi.org/10.1007/BF00320965

Beccaluva, L., & Serri, G. (1988). Boninitic and low-Ti subduction-related lavas from intraoceanic arc back arc systems and low-Ti ophiolites – a reappraisal of their petrogenesis and original tectonic setting. *Tectonophysics, 146*, 291-315. http://dx.doi.org/10.1016/0040-1951(88)90097-2

Beccaluva, L., Coltorti, M., Giunta, G., & Siena, F. (2004). Tethyan vs Cordilleran ophiolites: a reappraisal of distinctive tectonomagmatic features of supra-subduction complexes in relation to the subduction mode. *Tectonophysics, 393*, 163-174. http://dx.doi.org/10.1016/j.tecto.2004.07.034

Bedard, J. H. (2006). A catalytic delamination-driven model for coupled genesis of Archean crust and sub-continental lithospheric mantle. *Geochimica et Cosmochimica Acta, 70*, 1188-1214. http://dx.doi.org/10.1016/j.gca.2005.11.008

Bedard, J. H., Harris, L. B., & Thurston, P. (2013). The hunting of the snArc. *Precambrian Research, 229*, 20-48. http://dx.doi.org/10.1016/j.precamres.2012.04.001

Bell, D. R., Gregoire, M., Grove, T. L., Chatterjee, N., Carlson, R. W., & Buseck, P. R. (2005). Silica and volatile-element metasomatism of Archean mantle: a xenolith-scale example from the Kaapvaal craton. *Contributions to Mineralogy and Petrology, 150*, 251-267. http://dx.doi.org/10.1007/s00410-005-0673-8

Bibikova, E. V., Skiold, T., Bogdanova, S., Gorbatschev, R., & Slabunov, A. (2001). Titanite-rutile thermochronometry across the boundary between the Archaean Craton in Karelia and the Belomorian Mobile Belt, eastern Baltic Shield. *Precambrian Research, 105*, 315-330. http://dx.doi.org/10.106/S031-9268(00)00117-0

Bibikova, E. V., Bogdanova, S., Glebovitsky, V. A., Claesson, S., & Skiold, T. (2004). Evolution of the Belomorian Belt: NORDSIM U-Pb zircon dating of the Chupa paragneisses, magmatism, and metamorphic stages. *Petrology, 12*, 195-210.

Birkett, T. C., McCandless, T. E., & Hood, C. T. (2004). Petrology of the Renard igneous bodies: host rocks for diamond in the northern Otish Mountains region, Quebec. *Lithos, 76*, 475-490. http://dx.doi.org/10.1016/j.lithos.2004.03.054

Blichert, T. J., & Albarede, F. (1994). Short-lived chemical heterogeneities in the Archean mantle with implications for mantle convection. *Science, 263*, 1535-1540. http://dx.doi.org/10.1126/science.263.5153.1593

Blichert, T. J., & Albarede, F. (2008). Hafnium isotopes in Jack Hills zircons and the formation of the Hadean crust. *Earth and Planetary Science Letters, 265*, 686-702. http://dx.doi.org/10.1016/j.epsl2007.10.054

Bloomer, S. H., Stern, R. J., Fisk, E., & Geschwind, C. H. (1989). Shoshonitic volcanism in the Northern Mariana arc. 1. Mineralogic and major element trace element characteristics. *Journal of Geophysical Research, 94*, 4469-4496. http://dx.doi.org/10.1029/JB094iB04p04469

Bridgewater, D., Scott, D. J., Balagansky, V. V., Timmerman, M. J., Marker, M., Bushmin, S. A., … Daly, J. S. (2001). Age and provenance of early Precambrian metasedimentary rocks in the Lapland-Kola belt, Russia: evidence from Pb and Nd isotopic data. *Terra Nova, 13*, 32-37. http://dx.doi.org/10-1046/j.1365-3121.2001.00307x

Brooks, C., Ludden, J., Pigeon, Y., & Hubregtse, J. S. M. W. (1982). Volcanism of shoshonite to high-K andesite affinity in an Archean arc environment, Oxford Lake, Manitoba. *Canadian Journal of Earth Sciences, 19*, 55-67. http://dx.doi.org/10.1139/e82-005

Calcagnile, G. (1991). Deep structure of Fennoscandia from fundamental and higher mode dispersion of Rayleigh waves. *Tectonophysics, 195*, 139-149. http://dx.doi.org/10-106/0040-1951(91)90209-B

Cameron, W. E., McCulloch, M., & Walker, D. A. (1983). Boninite petrogenesis: chemical and Nd-Sr isotopic constraints. *Earth and Planetary Science Letters, 65*, 75-89. http://dx.doi.org/10.106/0012-821X(83)90191-7

Canil, D. (2008). Canada's craton: A bottoms-up view. *GSA Today, 18*, 4-10. http://dx.doi.org/10.1130/GSAT01806A.1.

Capdevila, R., Arndt, N., Letendre, J., & Sauvage, J. F. (1999). Diamonds in volcaniclastic komatiite from French Guiana. *Nature, 399*, 456-458. http://dx.doi.org/10.1038/20911

Carlson, R. W., & Boyet, M. (2008). Compositions of the earth's interior: the importance of early events. *Philosophical Transactions of the Royal Society of London, Series A, 366*, 4077-4103. http://dx.doi.org/10.1098/rsta.2008.0156

Chalapathi Rao, N. V. (2005). A petrological and geochemical reappraisal of the Mesoproterozoic diamondiferous Majhgawan pipe of Central India: Evidence for transitional kimberlite-orangeite (group II kimberlite)-lamproite rock type. *Mineralogy and Petrology, 84*, 69-106. http://dx.doi.org/10.1007/s00710-004-0072-2

Chalapathi Rao, N. V., Dongre, A., Kamde, G., Srivastava Rajesh, K., Sridar, M., & Kaminsky, F. V. (2010). Petrology, geochemistry and genesis of newly discovered Mesoproterozoic highly magnesian, calcite-rich kimberlites from Siddanpalli, Eastern Dharwar Craton, Southern India: products of subduction-related magmatic sources? *Mineralogy and Petrology, 98*, 313-328. http://dx.doi.org/10.1007/s00710-009-0085-4

Chiaradia, M., Muntener, O., & Beate, B. (2011). Enriched basaltic andesites from mid-crustal fraction crystallization, recharge, and assimilation (Pilavo volcano, Western Cordillera of Ecuador). *Journal of Petrology, 52*, 1107-1141. http://dx.doi.org/10.1093/petrology/egr020

Coleman, R. G. (1971). Plate tectonic emplacement of upper mantle peridotites along continental edges. *Journal of Geophysical Research, 76*, 1212-1222. http://dx.doi.org/10.1029/JB076i005.p01212

Condie, K. (2015). Changing tectonic settings through time: indiscriminate use of geochemical discriminant

diagrams. *Precambrian Research, 266*, 587-591. http://dx.doi.org/10.1016/j.precamres.2015.05.004

Condie, K. C., & Kroner, A. (2013). The building blocks of continental crust: evidence for a major change in the tectonic setting of continental growth at the end of the Archean. *Gondwana Research, 23*, 394-402. http://dx.doi.org/10.1016/j.gr.2011.09.011

Conticelli, S., Guarnieri, L., Farinelli, A., Mattei, M., Avanzinelli, R., Bianchini, G., … Venturelli, G. (2009). Trace element and Sr-Nd-Pb isotopes of K-rich, shoshonitic, and calc-alkaline magmatic associations in a post-collisional geodynamic setting. *Lithos, 107*, 68-92. http://dx.doi.org/10.1016/j.lithos.2008.07.016

Daly, J. S., Balagansky, V. V., Timmerman, M. S., Whitehouse, M. J., De Jong, K., Guise, P., … Bridgewater, D. (2001). Ion microprobe U-Pb zircon geochronology and isotopic evidence for a trans-crustal suture in the Lapland-Kola Orogen, northern Fennoscandian Shield. *Precambrian Research, 105*, 289-314. http://dx.doi.org/10.1016/SO301-9268(00)00116-9

Davies, G. F. (2006). Gravitational depletion of the early Earth's upper mantle and the viability of early plate tectonics. *Earth and Planetary Science Letters, 243*, 376-382. http://dx.doi.org/10.1016/j.epsl.2006.01.053

De Astis, G., Lucchi, F., Dellino, P., La Volpe, L., Tranne, C. A., Frezotti, M. L., & Peccerillo, A. (2013). Geology, volcanic history and petrology of Vulcano (central Aeolian archipelago). In Lucchi, F., Peccerillo, A., Keller, J., Tranne, C. A., & Rossi, P. L. (Eds.): *The Aeolian Islands Volcanoes (*pp. 281-349). London, United Kingdom: Geological Society of London Memoirs 37. http://dx.doi.org/10.1144/M37.11

Dhuime, B., Hawkesworth, C. J., Cawood, P., & Storey, C. D. (2012). A change in the geodynamics of continental growth 3 billion years ago. *Science, 335*, 1334-1336. http://dx.doi.org/10.1126/science.1216066

Digonnet, S., Goulet, N., Bourne, J., Stevenson, R., & Archibald, D. (2000). Petrology of the Abloviak aillikite dykes, New Quebec: evidence for a Cambrian diamondiferous alkaline province in northeastern North America. *Canadian Journal of Earth Sciences, 37*, 517-533. http://dx.doi.org/10.1139/e00-008

Dilek, Y., & Furnes, H. (2011). Ophiolite genesis and global tectonics: geochemical and tectonic fingerprinting of ancient oceanic lithosphere. *Geological Society of America Bulletin, 123*, 387-411. http://dx.doi.org/10.1130/B30446.1

Dostal, J., & Mueller, W. (1992). Archean shoshonites from the Abitibi greenstone belt, Chibougamau (Quebec, Canada): geochemistry and tectonic setting. *Journal of Volcanology and Geothermal Research, 53*, 145-165. http://dx.doi.org/10.1016/0377-0273(92)90079-S

Eldridge, C. S., Compston, W., Williams, I. S., Harris, J. W., & Bristow J. W. (1991). Isotope evidence for the involvement of recycled sediments in diamond formation. *Nature, 353*, 649-653. http://dx.doi.org/10.1038/353649aO

Eriksen, G. M. D. (2013). *Post-Precambrian magmatism in Eastern Finnmark, Norway: Mantle sources, possible origins and diamond potential*. M.Sci. Thesis, University of Tromso, Tromso, Norway, 75 p.

Ernst, W. G. (2009). Archean plate tectonics, rise of Proterozoic supercontinentality and onset of regional, episodic stagnant-lid behavior. *Gondwana Research, 15*, 243-253. http://dx.doi.org/10.1016/j.gr.2008.06.010

Foley, S. F., Buhre, S., & Jacob, D. E. (2003). Evolution of the Archean crust by delamination and shallow subduction. *Nature, 421*, 249-252. http://dx.doi.org/10.1038/nature01319

Francalanci, L., Luscchi, F., Keller, J., De Astis, G., & Tranne, C. A. (2013). Eruptive, volcano-tectonic and magmatic hitory of the Stromboli volcano (north-eastern Aeolian archipelago. In Lucchi, F., Peccerillo, A., Keller, J., Tranne, C. A., & Rossi, P. L. (Eds.): *The Aeolian Islands Volcanoes* (pp. 281-349). London, United Kingdom: Geological Society of London Memoirs 37. http://dx.doi.org/10.1144/M37.13

Frei, R., Polat, A., & Meibom, A. (2004). The Hadean upper mantle conundrum: evidence for source depletion and enrichment from Sm-Nd, Re-Os, and Pb isotopic compositions in 3.71 Gy boninite-like metabasalts from the Isua Supracrustal Belt, Greenland. *Geochimica et Cosmochimica Acta, 68*, 1645-1660. http://dx.doi.org/10.1016/j.gca.2003.10.009

Gaal, G., Berthersen, A., Gorbatschev, R., Kesola, R., Lehtonen, M. I., Marker, M., & Raase, P. (1989). Structure and composition of the Precambrian crust along the POLAR Profile in the northern Baltic Shield. *Tectonophysics, 162*, 1-25. http://dx.doi.org/10.1016/0040-1951(89)90354-5

Gill, J. B., & Whelan, P. (1989). Early rifting of an oceanic island arc (Fiji) produced shoshonitic to tholeiitic basalts. *Journal of Geophysical Research, 94*, 4561-4578. http://dx.doi.org/10.1029/JB094iB04904561

Gill, R. C. O., Aparicio, A., El Azzouzi, M., Hernandez, J., Thirlwall, M. F., Bourgois, J., & Marriner, G. F. (2004). Depleted arc volcanism in the Alboran Sea and shoshonitic volcanism in Morocco: geochemical and isotopic constraints on Neogene tectonic processes. *Lithos, 78*, 363-388. http://dx.doi.org/10.1016/j.lithos.2004.07.002

Golovko, A. V., & Kaminsky, F. V. (2010). The shoshonite-absarokite-picrite Karashoho pipe, Uzbekistan: an unusual diamond deposit in an atypical tectonic environment. *Economic Geology, 105*, 825-840. http://dx.doi.org/10.2113/gsecongeo.105.4.825

Gorbatschev, R., & Bogdanova, S. (1993). Frontiers in the Baltic Shield. *Precambrian Research, 64*, 3-21. http://dx.doi.org/10.1016/0301-9268(93)90066-B

Gurenko, A. A., & Kamenetsky, V. S. (2011). Boron isotopic composition of olivine-hosted melt inclusions from Gorgona komatiites, Colombia: new evidence supporting wet komatiite origin. *Earth and Planetary Science Letters, 312*, 201-212. http://dx.doi.org/10.1016/5.epsl.2011.09.033

Harris, L. B., & Bedard, J. H. (2014a). Crustal evolution and deformation in a non-plate-tectonic Archaean earth: Comparisons with Venus. In Y. Dilek & H. Furnes (Eds.): *Evolution of Archean Crust and Early Life* (pp. 249-264). Modern Approaches in Solid Earth Sciences 7. http://dx.doi.org/10.1007/978-94-007-7615-9_9

Harris, L. B., & Bedard, J. H. (2014b). Interactions between continent-like 'drift', rifting, and mantle flow on Venus – Gravity interpretations and Earth analogues. In Platz, T., Massironi, M., Byrne, P., & Hiesinger, H. H. (Eds.): *Volcanism and Tectonism Across the Solar System.* Geological Society of London Special Publication 401. http://dx.doi.org/10.1144/SP401.9.

Gurney, J. J., Helmstaedt, H. H., Richardson, S. H., & Shirey, S. B. (2010). Diamonds through time. *Economic Geology, 105*, 689-712. http://dx.doi.org/10.2113/gsecongeo.105.3.689

Harrison, T. M. (2009). The Hadean crust: evidence from > 4 Ga zircons. *Annual Reviews of Earth and Planetary Sciences, 37*, 479-505. http://dx.doi.org/10.1146/annurev.earth.031208.100151

Hastie, A. R., Mitchell, S. F., Kerr, A. C., Minifie, M. J., & Millar, I. L. (2011). Geochemistry of rare high-Nb basalt lavas: are they derived from a mantle wedge metasomatized by slab melts? *Geochimica et Cosmochimica Acta, 75*, 5049-5072. http://dx.doi.org/10.1016/j.gca.2011.06.018

Hawkesworth, C. J., Gallagher, K., Hergt, J., & McDermott, F. (1994). Destructive plate margin magmatism: geochemistry and melt generation. *Lithos, 33*, 169-188. http://dx.doi.org/10.1016/0024-4937(94)90059-0

Hoffmann, J. E., Munker, C., Polat, A., Konig, S., Mezger, K., & Rosing, M. T. (2010). Highly depleted Hadean mantle reservoirs in the sources of early Archean arc-like rocks, Isua supracrustal belt, southern West Greenland. *Geochimica et Cosmochimica Acta, 74*, 7236-7260. http://dx.doi.org/10.1016/j.gca.2010.09.027

Ireland, T. R., Rudnick, R. L., & Spetzius, Z. (1994). Trace elements in diamond inclusions from eclogites reveal link to Archean granites. *Earth and Planetary Science Letters, 128*, 199-213. http://dx.doi.org/10.1016/0012-821X(94)90145-7

Ishizuka, O., Yuasa, M., Tamura, Y., Shukuno, H., Stern, R. J., Naka, J., Joshima, M., & Taylor, R. N. (2010). Migrating shoshonitic magmatism tracks Izu-Bonin-Mariana intra-oceanic arc rift propagation. *Earth and Planetary Science Letters, 294*, 111-122. http://dx.doi.org/10.1016/j.epsl.2010.03.016

Ivanov, V. V., Kolesova, L. G., Khanchuk, A. I., Akatkin, V. N., Molchanova, G. B., & Nechaev, V. P. (2005). Find of diamond crystals in Jurassic rocks of the meymechite-picrite complex in the Sikhote-Alin orogenic belt. *Doklady Earth Sciences, 404*, 975-978.

Jaques, A. L., & Milligan, P. R. (2004). Patterns and controls on the distribution of diamondiferous intrusions in Australia. *Lithos, 77*, 783-802. http://dx.doi.org/10.1016/j.lithos.2004.03.042

Jenner, F. E., Bennett, V. C., Nutman, A. P., Friend, C. R. L., Norman, M. D., & Yaxley, G. (2009). Evidence for subduction at 3.8 Ga: geochemistry of arc-like metabasalts from the southern edge of the Isua Supracrustal Belt. *Chemical Geology, 261*, 83-98. http://dx.doi.org/10.1016/j.chemgeo.2008.09.016

Jolly, W. T. (1971). Potassium-rich igneous rocks from Puerto Rico. *Geological Society of America Bulletin, 82*, 399-408. http://dx.doi.org/10.1130/0016-7606(1971)82(399:pirfpr)2.0.CO;2

Joplin, G. A. (1968). The shoshonite association: a review. *Journal of Geological Society of Australia, 15*, 275-294. http://dx.doi.org/10.1080/00167616808728699

Jull, M., & Kelemen, P. B. (2001). On the conditions for lower crustal convective instability. *Journal of*

Geophysical Research, 106, 6423-6446. http://dx.doi.org/10.1029/2000JB900357

Ickert, R. B., Stachel, T., Stern, R. A., & Harris, J. W. (2013). Diamond from recycled crustal carbon documented by coupled d18O-d13C measurements of diamonds and their inclusions. *Earth and Planetary Science Letters, 364*, 85-97. http://dx.doi.org/10.1016/j.epsl.2013.01.008

Kamber, B. S. (2015). The evolving nature of terrestrial crust from the Hadean through the Archaean, into the Proterozoic. *Precambrian Research, 258*, 48-82. http://dx.doi.org/10.1016/j.precamres.2014.12.007

Kaminsky, F. V. (2007). Non-kimberlitic diamondiferous igneous rocks: 25 year on. *Journal of Geological Society of India, 69*, 557-575.

Kay, R. W. (1980). Volcanic arc magma genesis: implications for element recycling in the crust-upper mantle system. *Journal of Geology, 88*, 497-522. http://dx.doi.org/10.1086/628541

Kay, R. W., & Kay, S. M. (1993). Delamination and delamination magmatism. *Tectonophysics, 219*, 177-189. http://dx.doi.org/10.1016/0040-1951(93)90295-U

Keller, J. (1974). Petrology of some volcanic rocks series of the Aeolian Arc, Southern Tyrrhenian Sea: calc-alkaline and shoshonitic associations. *Contributions to Mineralogy and Petrology, 46*, 29-47. http://dx.doi.org/10.1007/BF00377991

Kepezhinskas, P. (1994). Diverse shoshonite magma series in the Kamchatka Arc: relationships between intra-arc extension and composition of alkaline magmas. In Smellie, J. L. (Ed.): *Volcanism Associated with Extension at Consuming Plate Margins* (pp. 249-264). Geological Society of London Special Publication 81. http://dx.doi.org/10.1144/GSL.SP.1994.081.01.14

Kepezhinskas, P. (2011a). Diamond exploration in eastern Finnmark. *Abstracts and Proceedings of the Geological Survey of Norway*, (1), 48-49.

Kepezhinskas, P. (2011b). Indicator minerals in diamond exploration: A case study from eastern Finnmark, Arkhangelsk and the Devonian Belt (Estonia, Lithuania, Novgorod, and Pskov). In McClenaghan, B., Peuraniemi, V. V., & Lehtonen, M. M. (Eds.). Rovaniemi, Finland: Proceedings of the 25th IAGS Workshop, pp. 7-11.

Kepezhinskas, P. K., Defant, M. J., & Drummond, M. S. (1996). Progressive enrichment of island arc mantle by melt-peridotite interaction inferred from Kamchatka xenoliths. *Geochimica et Cosmochimica Acta, 60*, 1217-1229. http://dx.doi.org/10.1016/0016-7037(96)00001-4

Kerrich, R., & Manikyamba, C. (2012). Contemporaneous eruption of Nb-enriched basalts- K-adakites-Na-adakites from the 2.7 Ga Penakacherla terrane: implications for subduction zone processes and crustal growth in the eastern Dharwar craton, India. *Canadian Journal of Earth Sciences, 49*, 615-636. http://dx.doi.org/10.1139/e2012-005

Kerrich, R., Wyman, D., Fan, J., & Bleeker, C. (1998). Boninite series: low Ti-tholeiite associations from the 2.7 Ga Abitibi greenstone belt. *Earth and Planetary Science Letters, 164*, 303-316. http://dx.doi.org/10.1016/S0012-821X(98)00223-4

Kjarsgaard, B. A. (2007). Kimberlite diamond deposits. In Goodfellow, W. D. (Ed.): *Mineral Deposits of Canada: A Synthesis of Major Deposit Types, DistrictMetallogeny, the Evolution of Geological Provinces, and Exploration Methods* (pp. 245-272). Geological Association of Canada, Mineral Deposits Division, Special Publication 5. http://dx.doi.org/10.2113/gsecongeo.102.7.1355

Konig, S., Munker, C., Schuth, S., Luguet, A., Hoffmann, J. E., & Kuduon, J. (2010). Boninites as windows into trace element mobility in subduction zones. *Geochimica et Cosmochimica Acta, 74*, 684-704. http://dx.doi.org/10.2113/gsecongeo.102.7.1355

Kontak, D. J., Clark, A. H., Farrar, E., Pearce, T. H., Strong, D. F., & Baadsgaard, H. (1986). Petrogenesis of a Neogene shoshonitic suite, Cerro Moromoroni, Puno, Southeastern Peru. *Canadian Mineralogist, 24*, 117-135.

Korikovsky, S. P., Kotov, A. B., Sal'nikova, E. B., Aranovich, L. Ya, Korpechkov, D. I., Yakovleva, S. Z., … Anisimova, I. V. (2014). The age of protolith of metamorphic rocks in the southeastern part of the Lapland granulite belt, southern Kola Peninsula: correlation with the Belomorian mobile belt in the context of the problem of Archean eclogites. *Petrology, 22*, 91-108. http://dx.doi.org/10.1134/S0869591114020040

Korja, A., Lahtinen, R., & Nironen, M. (2006). The Svecofennian orogeny: a collage of microcontinents and island arcs. *Geological Society of London Memoirs, 32*(1), 561-578.

Kusky, T. M., & Polat, A. (1999). Growth of granite-greenstone terranes at convergent margins and stabilization of Archean cratons. *Tectonophysics, 305*, 43-73. http://dx.doi.org/10.1144/GSL.MEM.2006.032.01.34

Kusky, T. M., Windley, B. F., Safonova, I., Wakita, K., Wakabayashi, J., Polat, A., & Santosh, M. (2013). Recognition of ocean plate stratigraphy in accretionary orogens through Earth history: a record of 3.8 billion years of sea floor spreading, subduction and accretion. *Gondwana Research 24*, 501-547. http://dx.doi.org/10.1144/GSL.MEM.2006.032.01.34

Leslie, R. A. J., Danyushevsky, L. V., Crawford, A. J., & Verbeeten, A. C. (2009). Primitive shoshonites from Fiji: geochemistry and source components. *Geochemistry, Geophysics, Geosystems, 10*, http://dx.doi.org/10.1029/2008GC002326.

Levchenkov, O. A., Levsky, L. K., Nordgulen, O., Dobrzhinetskaya, L. F., Vetrin, V. R., Cobbing, J., … Sturt, B. A. (1995). U-Pb zircon ages from Sør-Varanger, Norway, and the western part of the Kola Peninsula, Russia. *Norges Geologiske Undersokelse Special Publication, 7*, 29-47.

Logvinova, A. M., Taylor, L. A., Fedorova, E. N., Yelisseyev, A. P., Wirth, R., Howarth, G., Reutsky, V. N., & Sobolev, N. V. (2015). A unique diamondiferous peridotite xenoliths from the Udachnaya kimberlite pipe, Yakutia: role of subduction in diamond formation. *Russian Geology and Geophysics, 56*, 306-320. http://dx.doi.org/10.1016/j.rgg.2015.01.022

MacRae, N. D., Armitage, A. E., Jones, A. L., & Miller, A. R. (1995). A diamondiferous lamprophyre dike, Gibson Lake area, Northwest Territories. *International Geology Review, 37*, 212-229. http://dx.doi.org/10.1080/00206819509465401

Manikyamba, C., Kerrich, R., Khanna, T. C., Keshav Krishna, A., & Satyanarayanan, M. (2008). Geochemical systematics of komatiite-tholeiite and adakitic-arc basalt associations: The role of a mantle plume and convergent margin in formation of the Sandur Superterrane, Dharwar craton, India. *Lithos, 106*, 155-172. http://dx.doi.org/10.1016/j.lithos.2008.07.003

Manikyamba, C., Kerrich, R., Khanna, T. C., Satyanarayanan, M., & Keshav Krishna, A. (2009). Enriched and depleted arc basalts, with Mg-andesites and adakites: A potential paired arc-back-arc of the 2.6 Ga Hutti greenstone terrane, India. *Geochimica et Cosmochimica Acta, 73,* 1711-1736. http://dx.doi.org/10.1016/j.gca.2008.12.020

Manikyamba, C., Kerrich, R., Polat, A., Raju, K., Satyanarayanan, M., & Krishna, A. K. (2012). Arc picrite-potassic adakitic-shoshonitic volcanic association of the Neoarchean Sigegudda greenstone terrane, western Dharwar craton: transition from arc wedge to lithospheric melting. *Precambrian Research, 212-213*, 207-224. http://dx.doi.org/10.1016/j.precamres.2012.05.006

McCulloch, M. K., & Gamble, J. A. (1991). Geochemical and geodynamic constraints on subduction zone magmatism. *Earth and Planetary Science Letters, 102*, 358-374. http://dx.doi.org/10.1016/0012-821X(91)90029-H

McDonough, W. F., & Sun, S. S. (1995). The composition of the Earth. *Chemical Geology, 120*, 223-253. http://dx.doi.org/10.1016/0009-2541(94)00140-4

Meen, J. K. (1989). Formation of shoshonites from calcalkaline basaltic magmas: geochemical and experimental constraints from the type locality. *Contributions to Mineralogy and Petrology, 97*, 333-351. http://dx.doi.org/10.1007/BF0037199

Melezhik, V. A., & Sturt, B. (1994). General geology and evolutionary history of the early Proterozoic Polmak-Pasvik-Pechenga-Imandra/Varzuga-Ust'Ponoy Greenstone Belt in the northeastern Baltic Shield. *Earth-Science Reviews, 36*, 205-241. http://dx.doi.org/10.1016/0012-8252(94)90058-2

Melluzo, L., Morra, V., Guarino, V., De'Gennaro, R., Franciosi, L., & Grifa, C. (2014). The crystallization of shoshonitic to peralkaline trachyphonolitic magmas in a H_2O-Cl-F-rich environment at Ischia (Italy), with implications for the feeder system of the Campania Plain volcanoes. *Lithos, 210-211*, 242-259. http://dx.doi.org/10.1016/j.lithos.2014.10.002

Michaut, C., Jaupart, C., & Mareschal, J. C. (2009). Thermal evolution of cratonic roots. *Lithos, 109*, 47-60. http://dx.doi.org/10.1016/j.lithos.2008.05.008

Mints, M. V., Belousova, E. A., Konilov, A. N., Natapov, L. M., Shchipansky, A. A., Griffin, W. L., … Kaulina, T. V. (2010). Mesoarchean subduction processes: 2.87 Ga eclogites from the Kola Peninsula, Russia. *Geology, 38*, 739-742. http://dx.doi.org/10.1130/G31219.1

Miyashiro, A. (1974). Volcanic rock series in island arcs and active continental margins. *American Journal of Science, 274*, 321-355. http://dx.doi.org/10.2475/ajs.274.4.321

Miyashiro, A. (1975). Classification, characteristics, and origin of ophiolites. *Journal of Geology, 83*, 249-281. http://dx.doi.org/10.1086/628085

Mohapatra. R. K., & Honda, M. (2006). "Recycled" volatiles in mantle-derived diamonds – evidence from nitrogen and noble gas isotopic data. *Earth and Planetary Science Letters, 252*, 215-219. http://dx.doi.org/10.1016/j.epsl.2006.09.025

Morris, J., & Hart, S. R. (1983). Isotopic and incompatible element constraints on the genesis of island arc volcanics from Cold Bay and Amak Island, Aleutians, and implications for mantle structure. *Geochimica et Cosmochimica Acta, 47*, 2015-2030. http://dx.doi.org/10.1016/0016-7037(86)90202-4

Moores, E. M., & Vine, F. J. (1971). The Troodos massif, Cyprus, and other ophiolites as oceanic crust: evaluation and implications. *Philosophical Transactions of the Royal Society of London Series A, 268*, 443-466. http://dx.doi.org/10.1098/rsta.1971.0006

Moyen, J. F., Stevens, G., & Kisters, A. (2006). Record of mid-Archean subduction from metamorphism in the Barberton terrain, South Africa. *Nature, 442*, 559-562. http://dx.doi.org/10.1038/nature04972

Mueller, P. A., Wooden, J. L., Mogk, D. W., Henry, D. J., & Bowes, D. R. (2010). Rapid growth of an Archean continent by arc magmatism. *Precambrian Research, 183*, 70-88. http://dx.doi.org/10.1016/j.precamres.2010.07.013

Naqvi, S. M., Khan, R. M. K., Manikyamba, C., Mohan, R. M., & Khanna, T. C. (2006). Geochemistry of the Neoarchaean high-Mg basalts, boninites and adakites from the Kushtagi-Hungund greenstone belt of the Eastern Dharwar Craton (EDC): implications for the tectonic setting. *Journal of Asian Earth Sciences, 27*, 25-44. http://dx.doi.org/10.1016/j.jseaes.2005.01.006

Nemchin, A. A., Whitehouse, M. J., Menneken, M., Geister, Th., Pidgeon, R. T., & Wilde, S. (2008). A light carbon reservoir recorded in zircon-hosted diamond from the Jack Hills. *Nature, 454*, 92-95. http://dx.doi.org/10.1038/nature07102

Nesbitt, R. W., Sun, S. S., & Purvis, A. C. (1979). Komatiites: geochemistry and genesis. *Canadian Mineralogist, 17*, 165-186.

Nesterova, N. S., Kirnozova, T. I., & Fugzan, M. M. (2011). New U-Pb titanite age data on the rocks from the Karelian craton and the Belomorian mobile belt, Fennoscandian Shield. *Geochemistry International, 49*, 1161-1167. http://dx.doi.org/10.1134/S0016702911120081

Nielsen, T. F. D., Jensen, S. M., Secher, K., & Sand, K. K. (2009). Distribution of kimberlite and aillikite in the Diamond Province of southern West Greenland: a regional perspective based on groundmass mineral chemistry and bulk compositions. *Lithos, 112S*, 358-371. http://dx.doi.org/10.1016/j.lithos.2009.05.035

Niu, Y., & O'Hara, M. J. (2003). Origin of ocean island basalts: a new perspective from petrology, geochemistry, and mineral physics considerations. *Journal of Geophysical Research, 108*, 2209-2223. http://dx.doi.org/10.1029/2002JB002048.

Nutman, A. P., Bennett, V. C., & Friend, C. R. L. (2015). Proposal for a continent 'Itsaqia' amalgamated at 3.66 Ga and rifted apart from 3.53 Ga: Initiation of a Wilson Cycle near the start of the rock record. *American Journal of Science, 315*, 509-536. http://dx.doi.org/10.2475/06.2015.01

O'Neil, J., Carlson, R. W., Francis, D., & Stevenson, R. K. (2008). Neodimium-142 evidence for Hadean mafic crust. *Science, 321*, 1828-1831. http://dx.doi.org/10.1126/science.1161925

O'Neil, J., Francis, D., & Carlson, R. W. (2011). Implications of the Nuvvuagittuq Greenstone Belt for the formation of Earth's early crust. *Journal of Petrology, 52*, 985-1009. http://dx.doi.org/10.1093/petrology/egr014

Parmann, S. W., Grove, T. L., & Dann, J. C. (2001). The production of Barberton komatiites in an Archean subduction zone. *Geophysical Research Letters, 28*, 2513-2516. http://dx.doi.org/10.1029/2000GL012713

Pasquale, V., Verdoya, M., & Chiozzi, P. (2001). Heat flux and seismicity in the Fennoscandian Shield. *Physics of the Earth and Planetary Interior, 126*, 147-162. http://dx.doi.org/10.1016/S0031-9201(01)00252-7

Paulick, H., Bach, W., Godard, M., De Hoog, J. C. M., Suhr, G., & Harvey, J. (2006). Geochemistry of abyssal peridotites (Mid-Atlantic Ridge, 15°20'N, ODP Leg 209): implications for fluid/rock interaction in slow

spreading environments. *Chemical Geology, 234*, 179-210. http://dx.doi.org/10.1016/j.chemgeo.2006.04.011

Pearce, J. A. (2008). Geochemical fingerprinting of oceanic basalts with applications to ophiolite classification and the search for Archean oceanic crust. *Lithos, 100*, 14-48. http://dx.doi.org/10.1016/j.lithos.2007.06.016

Pearson, D. G., Snyder, G. A., Shirey, S. B., Taylor, L. A., Carlson, R. W., & Sobolev, N. V. (1995). Archean Re-Os age for Siberian eclogites and constraints on Archaean tectonics. *Nature, 374*, 711-713. http://dx.doi.org/10.1038/374711a0

Pe Piper, G. (1980). Geology and geochemistry of the Miocene shoshonitic suite of Lesbos, Greece. *Contributions to Mineralogy and Petrology, 72*, 387-396. http://dx.doi.org/10.1007/BF00371346

Pe Piper, G. (1983). Zoned pyroxenes from shoshonite lavas of Lesbos, Greece: inferences concerning shoshonite petrogenesis. *Journal of Petrology, 25*, 453-472. http://dx.doi.org/10.1093/petrology/25.2.453

Perfit, M. R., Gust, D. A., Bence, A. E., Arculus, R. J., & Taylor, S. R. (1980). Chemical characteristics of island-arc basalts – implications for mantle sources. *Chemical Geology, 15*, 684-704. http://dx.doi.org/10.1016/0009-2541(80)90107-2

Plank, T., & Langmuir, C. H. (1998). The chemical composition of subducting sediment and its consequences for the crust and mantle. *Chemical Geology, 145*, 325-394. http://dx.doi.org/10.1016/S0009-2541(97)00150-2

Platt, R. G., & Mitchell, R. H. (1982). The Marathon dikes: ultrabasic lamprophyres from the vicinity of McKellar Harbour, N.W.Ontario. *American Mineralogist, 67*, 907-916.

Polat, A., & Kerrich, R. (2001). Magnesian andesites, Nb-enriched basalts-andesites and adakites from late Archean 2.7 Ga Wawa greenstone belts, superior Province, Canada: implications for Late Archean subduction zone petrogenetic processes. *Contributions to Mineralogy and Petrology, 141*, 36-52. http://dx.doi.org/10.1007/s004100000223

Polat, A., & Kerrich, R. (2002). Nd-isotope systematics of ~2.7 Ga adakites, magnesian andesites, and arc basalts, Superior Province: evidence for shallow crustal recycling at Archean subduction zones. *Earth and Planetary Science Letters, 202*, 345-360. http://dx.doi.org/10.1016/S0012-821X(02)00806-3

Polat, A., & Munker, C. (2004). Hf-Nd isotope evidence for contemporaneous subduction processes in the source of late Archean arc lavas from the Superior Province, Canada. *Chemical Geology, 213*, 403-429. http://dx.doi.org/10.1016/j.chemgeo.2004.08.016

Polat, A., Hofmann, A. W., & Rosing, M. T. (2002). Boninite-like volcanic rocks in the 3.7-3.8 Ga Isua greenstone belt, West Greenland: geochemical. http://dx.doi.org/10.1016/S0009-2541(01)00363-1

Polat, A., Appel, P. W. U., & Fryer, B. J. (2011). An overview of the geochemistry of Eoarchean to Mesoarchean ultramafic to mafic volcanic rocks, SW Greenland: implications for mantle depletion and petrogenetic processes at subduction zones in the early Earth. *Gondwana Research, 20*, 255-283. http://dx.doi.org/10.1016/j.gr.2011.01.007

Puchtel, I. S., Hofmann, A. W., Amelin Yu, V., Garbe Schonberg, C. D., Samsonov, A. V., & Shchipansky, A. A. (1999). Combined mantle plume-island arc model for the formation of the 2.9 Ga Sumozero-Kenozero greenstone belt, SE Baltic Shield: isotope and trace element constraints. *Geochimica et Cosmochimica Acta,, 63*, 3579-3595. http://dx.doi.org/10.1016/S0016-7037(99)00111-8

Richardson, S. H., Shirey, S. B., Harris, J. W., & Carlson, R. W. (2001). Archean subduction recorded by Re-Os isotopes in eclogitic sulfide inclusions in Kimberley diamonds. *Earth and Planetary Science Letters, 191*, 257-266. http://dx.doi.org/10.1016/S0012-821X(01)00419-8

Roberts, D., & Nordgulen, Ø. (Eds.) (1995). Geology of the eastern Finnmark – western Kola Peninsula region. Special Publication 7, Norwegian Geological Survey NGU.

Robin Popieul, C. C. M., Arndt, N. T., Chauvel, C., Byerly, G., Sobolev, A. V., & Wilson, A. (2012). A new model for Barberton komatiites: deep critical melting with high retention. *Journal of Petrology, 53*, 2191-2229. http://dx.doi.org/10.1093/petrology/egs042

Rudnick, R. L., McDonough, W. F., & O'Connell, R. J. (1998). Thermal structure, thickness and composition of continental lithosphere. *Chemical Geology, 145*, 395-411. http://dx.doi.org/10.1016/S0009-2541(97)00151-4

Sajeev, K., Windley, B. F., Hegner, E., & Komiya, T. (2013). High-temperature, high-pressure granulites

(retrogressed eclogites) in the central region of the Lewisian, NW Scotland: crustal-scale subduction in the Neoarchean. *Gondwana Research, 23*, 526-538. http://dx.doi.org/10.1016/j.gr.2012.05.002

Sajona, F. G., Maury, R. C., Bellon, H., Cotton, J., & Defant, M. J. (1996). High field strength element enrichment of Pliocene-Pleistocene island arc basalts, Zamboanga, Western Mindanao (Philippines). *Journal of Petrology, 37*, 693-726. http://dx.doi.org/10.1093/petrology/37.3.693

Schulze, D. J., Harte, B., Valley, J. W., & De Channer, R. D. M. (2004). Evidence of subduction and crust-mantle mixing from a single diamond. *Lithos, 77*, 349-358. http://dx.doi.org/10.1016/j.lithos.2004.04.022

Serri, G. (1981). The petrochemistry of ophiolite gabbroic complexes. A key for classification of ophiolites into low-Ti and high-Ti types. *Earth and Planetary Science Letters, 52*, 203-212. http://dx.doi.org/10.1016/0012-821X(81)90221-1

Shchipansky, A. A., Khodorevskaya, L. I., & Slabunov, A. I. (2012). The geochemistry of and isotopic age of eclogites from the Belomorian Belt (Kola Peninsula): evidence for subducted Archean oceanic crust. *Russian Geology and Geophysics, 53*, 262-280. http://dx.doi.org/10.1016/j.rgg.2012.02.004

Shirey, S. B., & Richardson, S. H. (2011). Start of the Wilson cycle at 3 Ga shown by diamonds from sub-continental mantle. *Science, 333*, 434-436. http://dx.doi.org/10.1126/science.1206275

Shirey, S. B., Harris, J. W., Richardson, S. H., Fouch, M. J., James, D. E., Cartigny, P., … Viljoen, F. (2002). Diamond genesis, seismic structure, and evolution of the Kaapvaal-Zimbabwe craton. *Science, 297*, 1683-1686. http://dx.doi.org/10.1126/science.1072384

Shirey, S. B., Richardson, S. H., & Harris, J. W. (2004). Integrated models of diamond formation and craton evolution. *Lithos, 77*, 923-944. http://dx.doi.org/10.1016/j.lithos.2004.04.018

Shirey, S. B., Kamber, B. S., Whitehouse, M. J., Mueller, P. A., & Basu, A. R. (2008). A review of the isotopic and trace element evidence for mantle and crustal processes in the Hadean and Archean: implications for the onset of plate tectonic subduction. In Condie, K. C. & Pease, V. (Eds.): *When Did Plate Tectonics Begin on Planet Earth?* (pp. 129-148). Denver, Colorado: Geological Society of America Special Paper 440. http://dx.doi.org/10.1130/2008.2440(01)

Shu, Q., Brey, G. P., Hoefer, H. E., Zhao, Zh., & Pearson, D. G. (2016). Kyanite/corundum eclogites from the Kaapvaal Craton: subducted troctolites and layered gabbros from the Mid- to Early Archean. *Contributions to Mineralogy and Petrology, 171*, 11-35. http://dx.doi.org/10.1007/s00410-015-1225-5

Slabunov, A. I., Lobach Zhuchenko, S. B., Bibikova, E. V., Balagansky, V. V., Sorjonen Ward, P., Volodichev, O. I., … Stepanov, V. S. (2006). The Archean of the Baltic Shield: geology, geochronology, and geodynamic settings. *Geotectonics, 40*, 409-433. http://dx.doi.org/10.1134/S001685210606001X

Sloman, L. E. (1989). Triassic shoshonites from the Dolomites, northern Italy: alkaline arc rocks in a strike-slip setting. *Journal of Geophysical Research, 94*, 4655-4666. http://dx.doi.org/10.1029/JB094iB04p04655

Smelov, A. P., Shatsky, V. S., Ragozin, A. L., Reutskii, V. N., & Molotkov, A. E. (2012). Diamondiferous Archean rocks of the Olondo greenstone belt (western Aldan-Stanovoy shield). *Russian Geology and Geophysics, 53*, 1012-1022. http://dx.doi.org/10.1016/j.rgg.2012.08.005

Smith, C. B., Haggerty, S. E., Chatterjee, B., Beard, A., & Townend, R. (2013). Kimberlite, lamproite, ultramafic lamprophyre and carbonate relationships on the Dharwar Craton, India: an example from the Khaderpet pipe, a diamondiferous ultramafic with associated carbonatite intrusion. *Lithos, 182-183*, 102-113, http://dx.doi.org/10.1016/j.lithos.2013.10.006

Smithies, R. H., Champion, D. C., & Sun, S. S. (2004). The case for Archean boninites. *Contributions to Mineralogy and Petrology, 147*, 705-725. http://dx.doi.org/10.1007/s00410-004-0579-x

Smithies, R. H., Champion, D. C., Van Kranendonk, M. J., Howard, H. M., & Hickman, A. (2005). Modern-style subduction processes in the Mesoarchean: geochemical evidence from the 3.12 Ga Whundo intra-oceanic arc. *Earth and Planetary Science Letter, 213*, 221-237. http://dx.doi.org/10.1016/j.epsl.2004.12.026

Smithies, R. H., Van Kranendonk, M. J., & Champion, D. C. (2007). The Mesoarchean emergence of modern-style subduction. *Gondwana Research, 11*, 50-68. http://dx.doi.org/10.1016/j.gr.2006.02.001

Spandler, C., & Pirard, C. (2013). Element recycling from subducting slabs to arc crust: a review. *Lithos, 170-171*, 208-223. http://dx.doi.org/10.1016/j.lithos.2013.02.016

Stachel, T., & Harris, J. W. (2008). The origin of cratonic diamonds – constraints from mineral inclusions. *Ore*

Geology Reviews, 34, 5-32. http://dx.doi.org/10.1016/j.oregeorev.2007.05.002

Stachel, T., Harris, J. W., & Muehlenbachs, K. (2009). Sources of carbon in inclusion bearing diamonds. *Lithos, 112S*, 625-637. http://dx.doi.org/10.1016/j.lithos.2009.04.017

Stern, R. J. (2002). Evidence from ophiolites, blueschists, and ultrahigh-pressure metamorphic terranes that the modern episode of subduction tectonics began in Neoproterozoic time. *Geology, 33*, 557-560. http://dx.doi.org/10.1130/G21365.1

Sun, S. S., & McDonough, W. F. (1989). Chemical and isotope systematics of oceanic basalts: implications for mantle composition and process. In Saunders, A. D. & Norry, M. J. (Eds.). *Magmatism in the Ocean Basins* (pp. 818-845). London, United Kingdom: Geological Society of London Special Publication 42. http://dx.doi.org/10.1144/GSL.SP.1989.042.01.19

Sun, C. H., & Stern, R. J. (2001). Genesis of Mariana shoshonites: contribution of the subduction component. *Journal of Geophysical Research, 106*, 589-608. http://dx.doi.org/10.1029/2000JB900342

Sun, C. H., Stern, R. J., Yoshida, T., & Kimura, J. I. (1998). Fukutoku-oka-no-ba Volcano: a new perspective on the alkali volcano province in the Izu-Bonin-Mariana arc. *The Island Arc, 7*, 432-442. http://dx.doi.org/10.1111/j.1440-1738.1998.t01-1-00201.x

Szilas, K., Naeraa, T., Schersten, A., Stendal, H., Frei, R., Van Hinsberg, V. J., … Rosing, M. T. (2012a). Origin of Mesoarchean arc-related rocks with boninite/komatiite affinities from southern West Greenland. *Lithos, 144-145*, 24-39. http://dx.doi.org/10.1016/j.lithos.2012.03.023

Szilas, K., Hoffman, J. E., Schersten, A., Rosing, M. T., Windley, B. F., Kokfelt, T. F., … Munker, C. (2012b). Complex calc-alkaline volcanism recorded in Mesoarchean supracrustal belts north of Frederikshab Isblink, southern West Greenland: implications for subduction zone processes in the early Earth. *Precambrian Research, 208-211*, 90-123. http://dx.doi.org/10.1016/j.precamres.2012.03.013

Szilas, K., Van Hinsberg, V. J., Kisters, A. F. M., Hoffmann, J. E., Windley, B. F., Kokfelt, T. F., … Munker, C. (2013). Remnants of arc-related Mesoarchean oceanic crust in the Tartoq Group of SW Greenland. *Gondwana Research, 23*, 436-451. http://dx.doi.org/10.1016/j.gr.2011.11.006

Tappe, S., Foley, S. F., Kjarsgaard, B. A., Romer, R. L., Heaman, L. M., Stracke, A., & Jenner, G.A. (2008). Between carbonatite and lamproite – diamondiferous Torngat ultramafic lamprophyres formed by carbonate-fluxed melting of cratonic MARID-type metasomes. *Geochimica et Cosmochimica Acta, 72*, 3258-3286. http://dx.doi.org/10.1016/j.gca.2008.03.008

Tappe, S., Smart, K. A., Pearson, D. G., Steenfelt, A., & Simonetti, A. (2011a). Craton formation in Late Archean subduction zones revealed by first Greenland eclogites. *Geology, 39*, 1103-1106. http://dx.doi.org/10.1130/G32348.1

Tappe, S., Pearson, D. G., Nowell, G., Nielsen, T., Milstead, P., & Muehlenbachs, K. (2011b). A fresh look at Greenland kimberlites: cratonic mantle lithosphere imprint on deep source signal. *Earth and Planetary Science Letters, 305*, 235-248. http://dx.doi.org/10.1016/j.epsl.2011.03.005

Tatsumi, Y. (2000). Continental crust formation by crustal delamination in subduction zones and complementary accumulation of the enriched mantle I component in the mantle. *Geochemistry, Geophysics, Geosystems, 1*. http://dx.doi.org/10.1029/2000GC000094

Thirlwall, M. F., Smith, T. E., Graham, A. M., Theodorou, N., Hollings, P., Davidson, J. P., & Arculus, R. J. (1994). High field strength element anomalies in arc lavas: source or process? *Journal of Petrology, 35*, 819-838. http://dx.doi.org/10.1093/petrology/35.3.819

Thompson, R. N., & Fowler, M. B. (1986). Subduction-related shoshonitic and ultrapotassic magmatism: a study of Siluro-Ordovician syenites from the Scottish Caledonides. *Contributions to Mineralogy and Petrology, 94*, 507-522. http://dx.doi.org/10.1007/BF00376342

Timmerman, M. J., & Daly, J. S. (1995). Sm-Nd evidence for Late Archaean crust formation in the Lapland-Kola mobile belt, Kola Peninsula, Russia and Norway. *Precambrian Research, 72*, 97-107. http://dx.doi.org/10.1016/0301-9268(94)00045-S

Torsvik, T. H., Smethurst, M. A., Meert, J. G., Van Der Voo, R., McKerrow, W. S., Brasier, M. D., … Walderhaug, H. J. (1986). Continental break-up and collision in the Neoproterozoic and Palaeozoic – A tale of Baltica and Laurentia. *Earth-Science Reviews, 40*, 229-258. http://dx.doi.org/10.1016/0012-8252(96)00008-6

Turner, S., Rushmer, T., Reagan, M., & Moyen, J. F. (2014). Heading down early on? Start of subduction on Earth. *Geology, 42*, 139-142. http://dx.doi.org/10.1130/G34886.1

Weiss, Y., McNeill, J., Pearson, D. G., Nowell, G. M., & Ottley, C. J. (2015). Highly saline fluids from a subducting slab as the source for fluid-rich diamonds. *Nature, 524*, 339-342. http://dx.doi.org/10.1038/nature14857

Westerlund, K. J., Shirey, S. B., Richardson, S. H., Carlson, R. W., Gurney, J. J., & Harris, J. W. (2006). A subduction wedge origin for Paleoarchean peridotitic diamonds and harzburgites from the Panda kimberlite, Slave Craton: evidence from Re-Os isotope systematics. *Contributions to Mineralogy and Petrology, 152*, 275-294. http://dx.doi.org/10.1007/s00410-006-0101-8

Workman, R. K., & Hart, S. R. (2005). Major and trace element composition of the depleted MORB mantle (DMM). *Earth and Planetary Science Letters, 231*, 53-72. http://dx.doi.org/10.1016/j.epsl.2004.12.005

Wyman, D. A. (1999). A 2.7 Ga depleted tholeiite suite: evidence of plume-arc interaction in the Abitibi Greenstone Belt, Canada. *Precambrian Research, 97*, 27-42. http://dx.doi.org/10.1016/S0301-9268(99)00018-2

Wyman, D. A., & Kerrich, R. (1993). Archean shoshonitic lamprophyres of the Abitibi Sub-province, Canada: petrogenesis, age, and tectonic setting. *Journal of Petrology, 34*, 1067-1109. http://dx.doi.org/10.1093/petrology/34.6.1067

Wyman, D. A., Kerrich, R., & Polat, A. (2002). Assembly of Archean cratonic mantle lithosphere and crust: plume-arc interaction in the Abitibi-Wawa subduction-accretion complex. *Precambrian Research, 115*, 37-62. http://dx.doi.org/10.1016/S0301-9268(02)00005-0

Wyman, D. A., Ayer, J. A., Conceicao, R. V., & Sage, R. P. (2006). Mantle processes in an Archean orogeny: evidence from 2.67 Ga diamond-bearing lamprophyres and xenoliths. *Lithos, 89*, 300-328. http://dx.doi.org/10.1016/j.lithos.2005.12.005

Yang, W. B., Nin, H. C., Shan, Q., Luo, Y., Sun, W. D., Li, C. Y., … Yu, Y. Y. (2012). Late Paleozoic calc-alkaline to shoshonitic magmatism and its geodynamic implications, Yuximolegai area, western Tianshan, Xinjiang. *Gondwana Research, 22*, 325-340. http://dx.doi.org/10.1016/j.gr.2011.10.008

Zegers, T. E., & Van Keken, P. E. (2001). Middle Archean continent formation by crustal delamination. *Geology, 29*, 1083-1086. http://dx.doi.org/10.1130/0091-7613(2001)